Redox-Switchable Transfer Hydrogenations with P -Chiral Dendritic Ferrocenyl Phosphine Complexes

John Popp, Anne-Marie Caminade, Evamarie Hey-Hawkins

EurJIC
European Journal of Inorganic Chemistry

Full Paper
doi.org/10.1002/ejic.202000142

Redox-Switchable Dendrimers

Redox-Switchable Transfer Hydrogenations with *P*-Chiral Dendritic Ferrocenyl Phosphine Complexes

John Popp,[a] Anne-Marie Caminade,[b] and Evamarie Hey-Hawkins*[a]

Abstract: Attaining absolute control over a catalytic process and, therewith, exploiting its full potential pleases scientists in their ambitious and ongoing endeavor to perform catalysis like Nature does. In this regard, redox-switchable catalysis certainly holds great potential, constantly gaining importance in modern catalysis research. Herein, we report the application of *P*-stereogenic dendritic ferrocenyl phosphines in the ruthenium-catalyzed redox-switchable transfer hydrogenation of a ketone yielding an enantioenriched alcohol. By adding a chemical oxidant or reductant, the catalytic activity of the complexes was reversibly switched off and back on again over the course of the hydrogen transfer reaction. This has been rationalized mainly in terms of a distinct electronic communication between the redox-active group and the catalytic center. The highly functionalized dendritic catalysts presented here might impact the way prospective homogeneous catalysts will be designed.

Introduction

The concept of redox-switchable catalysis (RSC) is based on the incorporation of a redox-active functionality within a ligand framework allowing the catalytic activity of the coordinated transition metal to be controlled in situ.[1] Without changing the formal oxidation state of the metal, oxidation and reduction influence the electron-donating ability of the redox-active ligand and, thereby, the reactivity and/or selectivity of the catalyst.[2] A pioneering demonstration of this concept utilized a rhodium(I) bisphosphino cobaltocene complex displaying orthogonal activity in different reactions depending on its redox state. Thus, the same compound is a faster hydrosilylation catalyst in its oxidized form and a better hydrogenation catalyst in the reduced state.[3] This outstanding work laid the foundation for a spectacular development of RSC as an important area of homogeneous catalysis.[4–10] Although RSC has been applied to a wide variety of catalytic reactions, such as ring-opening polymerizations,[11–17] ring-closing metatheses[18,19] and other reactions,[20–27] surprisingly little attention has been devoted to the redox-controlled formation of alcohols by transfer hydrogenation (TH).[28] This is particularly remarkable, given that TH is an attractive alternative to direct hydrogenation and has recently become the center of research in hydrogenation science.[29]

The increasing success of TH[30–37] is due to the avoidance of hazardous pressurized H_2 gas, distinct reactivity and chemo- and enantioselectivity, the availability of inexpensive and easy to handle hydrogen donors and recyclability of the major side product. The formal transfer of two H atoms from a hydrogen donor to a carbonyl group in the presence of a catalyst is a key transformation in homogeneous catalysis, especially the asymmetric version (ATH),[38–42] since it frequently provides quantitative conversions and high enantioselectivities within reasonable reaction times. Major breakthroughs in ATH were marked by applying monotosylated 1,2-diamines,[43–47] and β-amino alcohols[48,49] as highly efficient ligands for the reduction of ketones. This tremendous success of nitrogen-containing donors generally overshadowed hydrogen transfers with phosphine-based ligands which is unexpected as they are routinely used in direct hydrogenations.[31]

Admittedly, early examples of phosphine ligands in ATH provided good conversions but their performance in terms of enantioselectivity was overall unsatisfactory.[50–52] Their application in ATH gained fresh momentum as more sophisticated methods for the preparation of *P*-stereogenic ligands were established.[53–55] In particular, stereoselective synthesis in the presence of chiral auxiliaries became the preferred strategy for synthesizing tertiary *P*-stereogenic phosphines due to the great versatility and stereoselectivity obtained by this methodology.[55] Consequently, a series of ruthenium complexes $[RuCl_2(arene)P^*]$ (P* = *P*-stereogenic monodentate phosphine) for ATH were developed,[56–59] of which some were immobilized on carbosilane dendrimers.[60]

Immobilization of catalytic entities on solid materials is an advancing approach in catalysis research to overcome an essential drawback of homogeneous catalysts, their limited recyclability. In contrast to insoluble supports, dendritic polymers

[a] *Faculty of Chemistry and Mineralogy, Institute of Inorganic Chemistry, Leipzig University, Johannisallee 29, 04103 Leipzig, Germany*
E-mail: hey@uni-leipzig.de
https://anorganik.chemie.uni-leipzig.de/de/anorganik/ak-hey-hawkins/
[b] *Laboratoire de Chimie de Coordination du CNRS, 205 Route de Narbonne, BP 44099, 31077 Toulouse Cedex 4, France*
Supporting information and ORCID(s) from the author(s) for this article are available on the WWW under https://doi.org/10.1002/ejic.202000142.

Full Paper
doi.org/10.1002/ejic.202000142

offer a well-defined molecular architecture allowing the precise control of the catalyst structure and are both soluble and recoverable by precipitation or nanofiltration.[61–63] Furthermore, high local concentrations of catalytic units located on the surface of dendrimers may cause dendritic effects where different activities, depending on whether they are linked to a dendrimer or not, or depending on the dendrimer generation, are observed.[64]

We have recently reported a positive dendritic effect (higher catalytic activity of the dendritic catalyst than its monomeric analog at the same metal loading) in the ruthenium-catalyzed isomerization of an allylic alcohol, which was also the first application of a dendritic transition metal complex in redox-switchable catalysis.[65] This remarkable demonstration of redox control of ferrocenyl phosphine ligands over the catalytically active transition metal encouraged us to introduce *P*-stereogenic ferrocenyl phosphines into the ligand system for asymmetric catalysis. Consequently, we herein report the preparation and electrochemical characterization of *P*-stereogenic dendritic ferrocenyl phosphine ligands with different substituents at the phosphorus atom, which were applied in the ruthenium-catalyzed asymmetric transfer hydrogenation. Furthermore, the incorporated ferrocenyl moiety allowed us to apply the concept of RSC to these reactions, electrochemically controlling the catalytic activity in situ.

Results and Discussion

Synthesis of *P*-Stereogenic Ferrocenyl Phosphines

A key step in the synthesis of phosphorus-containing dendrimers is the quantitative substitution of terminal P–Cl bonds by functionalized phenols.[66] Therefore, the immobilization of ferrocenyl phosphines on the surface of such dendrimers requires a free phenol function at one cyclopentadienyl ring, since only phenolic OH groups are reactive enough to substitute terminal P–Cl bonds quantitatively. Recently, we prepared three *P*-stereogenic ferrocenyl phosphine boranes **2a–c-ML** with a 4-methoxyphenyl substituent in the 1′-position of the ferrocenyl group (Scheme 1).[67,68]

In these monomeric (non-dendritic) ligands (**ML**) the 4-methoxyphenyl substituent serves to mimic the phenol linker which is needed in immobilization reactions. The *P*-stereogenic ferrocenyl phosphine boranes **2a–c-ML** were synthesized with excellent enantiopurity (> 95 % *ee* in all cases) and subsequent borane-deprotection by heating in diethylamine, followed by reaction with [{Ru(*p*-cymene)Cl_2}$_2$], yielded the monomeric ruthenium complexes **3a–c-ML-Ru**. Investigating ligands and complexes at the monomeric level prior synthesizing dendrimers, in general, allowed simplified purification and characterization procedures and provided crucial insights into complexation properties. Thus, we found that **3b-ML-Ru** undergoes a teth-

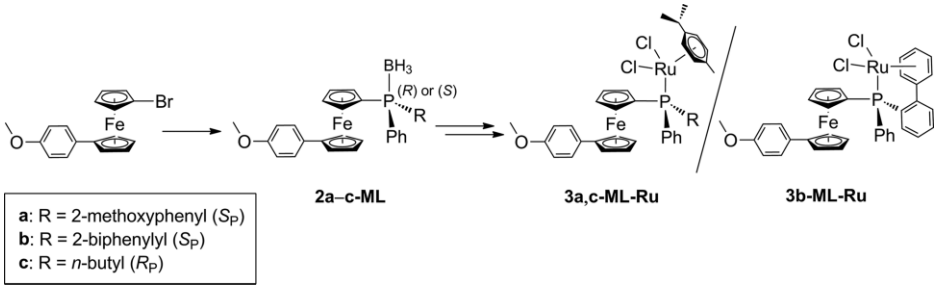

Scheme 1. Monomeric *P*-stereogenic ferrocenyl phosphine boranes **2a–c-ML** and their corresponding monomeric ruthenium complexes **3a–c-ML-Ru**. **3b-ML-Ru** forms a tethered complex with loss of the *p*-cymene ligand when activated by light.[67,68]

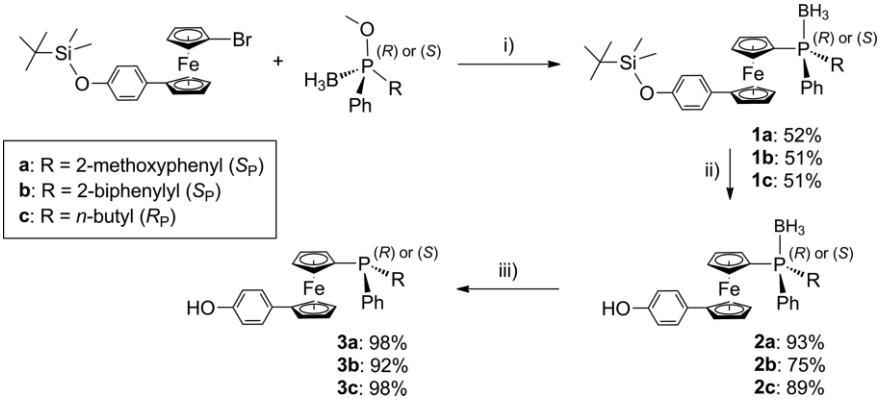

Scheme 2. Synthesis of the *P*-stereogenic ferrocenyl phosphines **3a–c**. i) *n*BuLi, –80 °C; ii) [nBu$_4$N]F·3H$_2$O; iii) NHEt$_2$, 50 °C.

ering process by replacing an η^6-coordinating arene ligand upon mild photochemical activation by a conventional desk lamp (Scheme 1).[67] Furthermore, the monomeric ruthenium complexes **3a–c-ML-Ru** were used for comparison in catalytic tests of the dendritic complexes identifying potential dendritic effects, whereby equal metal loadings must certainly be adhered.

To synthesize the corresponding dendritic ligands, the synthetic route for the monomeric compounds was slightly modified and 1-bromo-1′-[(4-phenoxy)*tert*-butyldimethylsilyl]-ferrocene[65,69] was treated with methyl (phenyl)phosphinite boranes (Scheme 2). These phosphinite boranes were synthesized by way of an (–)-ephedrine-based oxazaphospholidine borane complex[70] bearing different substituents at the phosphorus atom. At low temperature, the phosphinite boranes were treated with the lithiated ferrocenyl precursor affording the corresponding tertiary phosphine boranes **1a**–**c**, with inversion of configuration at the phosphorus atom, in good yields and excellent enantiomeric excesses (> 97 % *ee* in all cases). Exemplarily, the solid-state molecular structure of the fully protected ferrocene derivative **1a** showed the expected molecular features for these 1,1′-substituted ferrocenes with an *anti* arrangement (Figure 1).

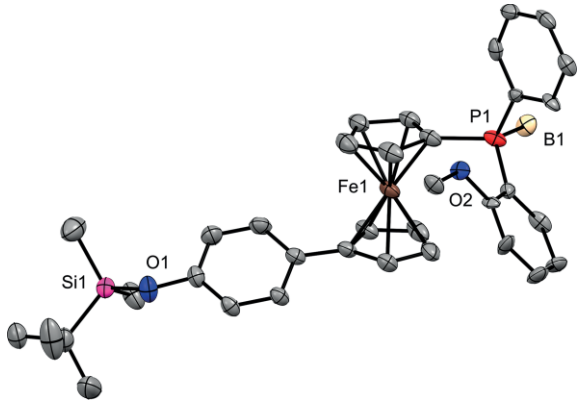

Figure 1. Molecular structure of **1a** in the solid state. Ellipsoids at 50 % probability; hydrogen atoms are omitted for clarity.

Deprotection of the silyl-protected phosphine boranes **1a**–**c** with tetra-*n*-butylammonium fluoride trihydrate gave the phenol-functionalized ferrocene derivatives **2a–c** in very good yields with preservation of enantiopurity. Finally, borane-deprotection was achieved by heating in diethylamine, yielding the free ferrocenyl phosphines **3a–c** in nearly quantitative yields. This step, again, fully retained the configuration at the phosphorus atom which was demonstrated by reprotection with BH_3•SMe_2 prior analysis by chiral HPLC (> 92 % *ee* in all cases).

Particular care should be taken during chromatographic purification of these *P*-stereogenic ferrocenyl phosphines since they tend to racemize on conventional silica or alumina, as we recently demonstrated.[68] The use of deactivated silica, pretreated by amine, prevented the racemization while retaining reasonable chromatographic resolution. The *P*-stereogenic ferrocenyl phosphines thus obtained represent ideal precursors for immobilized ligands exhibiting a free phenol function for immobilization at one cyclopentadienyl ring and a free phosphine for coordination at the other cyclopentadienyl ring of ferrocene.

Synthesis of Dendritic Ruthenium(II) Complexes

The phosphorus-containing dendrimers used for immobilization were constructed by divergent strategy by grafting concentric layers from the hexafunctional $N_3P_3Cl_6$ core, thus building up generation by generation.[71] Within this approach, $P(S)Cl_2$ groups act as branching functions in each generation, and each step in this reaction sequence gives quantitative conversion, which is a requirement in the synthesis of this kind of dendrimers. Due to the presence of phosphorus atoms in the core and in every branch of the dendritic architecture, $^{31}P\{^1H\}$-NMR spectroscopy is an indispensable technique for monitoring the reaction progress of every synthetic step.

The immobilization experiments were performed with generation one (**G_1**, Scheme 3) and generation two (**G_2**, Scheme 4) of phosphorus-containing dendrimers bearing 12 and 24 P–Cl terminal functions, respectively, and a slight excess of the ferrocenyl phosphines **3a–c**. As for the synthesis of the dendrimers, the reaction progress was, again, controlled by $^{31}P\{^1H\}$-NMR spectroscopy showing a characteristic chemical shift of the terminal phosphorus atom. With advancing substitution, the signal shifts from about δ = 63 [$P(S)Cl_2$] to around 70 ppm for mono substitution [P(S)Cl(O–aryl)], and to δ = 62 ppm for disubstitution [$P(S)(O\text{–aryl})_2$], thus giving distinct indication of the immobilization progress.

After filtration of cesium carbonate, the dendrimers were precipitated with *n*-pentane whereby the slight excess of ferrocenyl phosphine remained in solution and could therefore easily be separated by filtration. The obtained *P*-stereogenic dendritic ferrocenyl phosphines **3a–c-G_1** and **3a–c-G_2** were isolated in excellent yields, and characterization by $^{31}P\{^1H\}$-NMR spectroscopy confirmed their purity, exhibiting three signals: δ = –24 to –29 ppm for the terminal phosphines, depending on their structure, 8 ppm for the core and 62 ppm for branching phosphorus atoms.

In order to form dendritic heterobimetallic complexes, the dendritic phosphine ligands were reacted at room temperature with 0.5 equivalents of di-μ-chlorobis[(η^6-*p*-cymene)-chlororuthenium(II)] per terminal phosphine. In contrast to the corresponding monomeric complexes **3a–c-ML-Ru**, purification on silica could not be applied due to the size of the dendrimers. Alternatively, the dendritic complexes were purified by precipitation with hexane/CH_2Cl_2 (3:1). Thus, first-generation complexes **3a–c-G_1-Ru** (Scheme 3) and second-generation complexes **3a–c-G_2-Ru** (Scheme 4) were obtained in quasi-quantitative yields in almost all cases. Only the butyl-substituted dendritic complex was partially soluble in hexane/CH_2Cl_2 (3:1) resulting in a reduced yield of **3c-G_1-Ru**. Decreasing the polarity of the solvent mixture (hexane/CH_2Cl_2, 6:1) ensured an improved yield of **3c-G_2-Ru**.

Upon complexation, a characteristic low-field shift in the $^{31}P\{^1H\}$-NMR spectra for the terminal phosphines is observed, indicating successful coordination. Similar to the monomeric complex **3b-ML-Ru**, the 2-biphenylyl-substituted dendritic

Full Paper
doi.org/10.1002/ejic.202000142

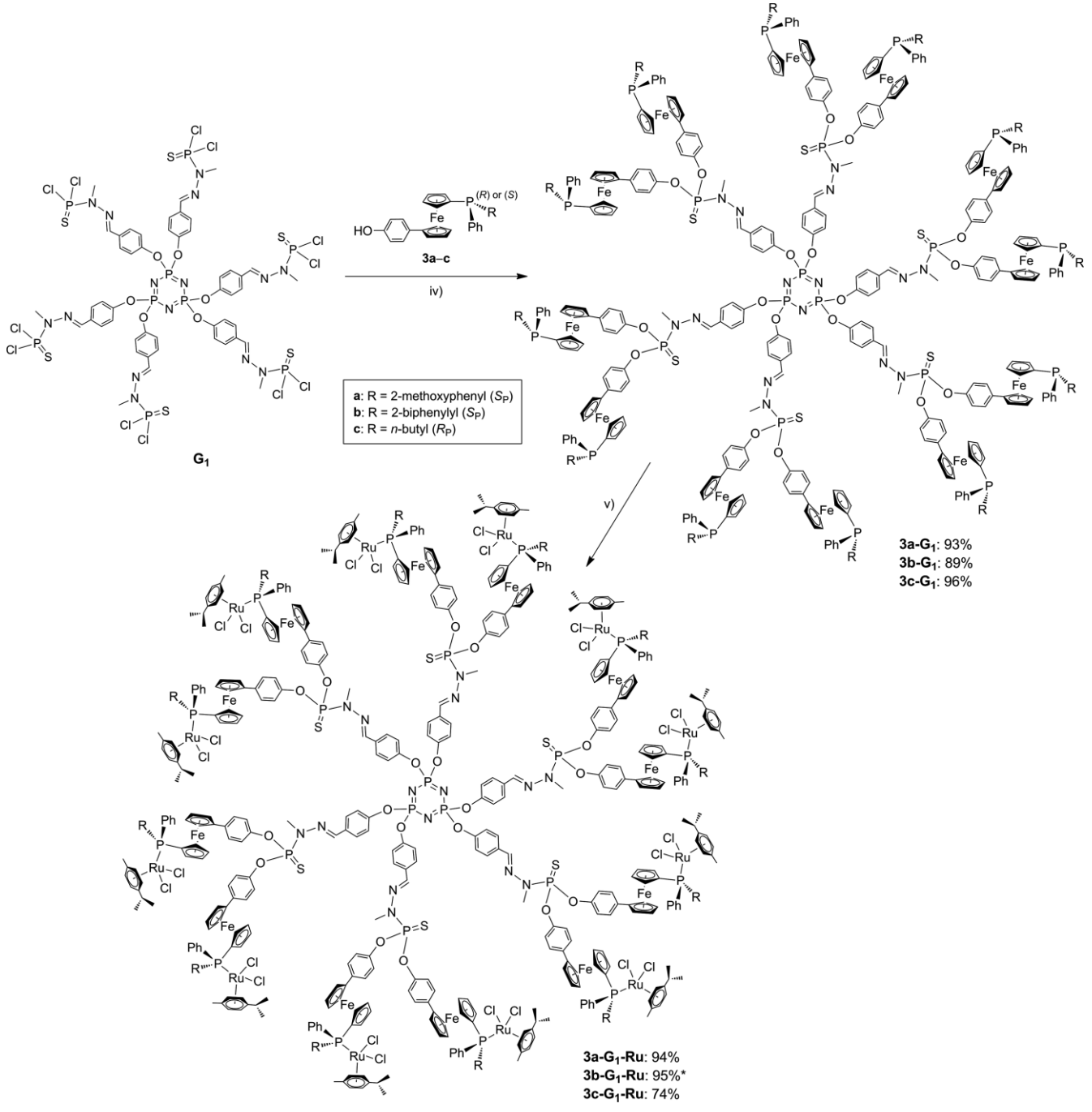

Scheme 3. Synthesis of the *P*-stereogenic dendritic ferrocenyl phosphine ruthenium complexes **3a–c-G_1-Ru**. iv) 12 equiv. **3a–c**, Cs_2CO_3, THF, r.t.; v) 6 equiv. [{Ru(*p*-cymene)Cl_2}$_2$], DCM, r.t. ***3b-G_1-Ru** forms a tethered complex with loss of the *p*-cymene ligand when activated by light.

complexes **3b-$G_{1,2}$-Ru** underwent a tethering process by replacing the η^6-coordinating *p*-cymene ligand when photochemically activated. The formation of this strained ruthenacycle shifts the phosphine signal in the $^{31}P\{^1H\}$-NMR spectra further downfield (δ = 43 ppm), in comparison to the dendritic complexes **3a-$G_{1,2}$-Ru** and **3b-$G_{1,2}$-Ru** (δ = 17 ppm and 15 ppm, respectively).

Electrochemistry

The monomeric and dendritic complexes were electrochemically investigated, primarily, to evaluate their suitability for redox-switched applications in catalysis. Therefore, distinctly separated redox processes for Fe^{2+}/Fe^{3+} and Ru^{2+}/Ru^{3+}, with the former being fully reversible, are required. The separation of these redox potentials constitutes the electrochemical window for prospective chemical oxidants affecting exclusively ferrocene units without interfering with the ruthenium redox process. Besides comparing monomeric (**ML-Ru**) and dendritic complexes (**$G_{1,2}$-Ru**), electrochemical experiments were furthermore performed to examine the influence of different phosphorus substituents (**3a–c**) on the redox potential of the ruthenium complexes (Figure 2).

Full Paper
doi.org/10.1002/ejic.202000142

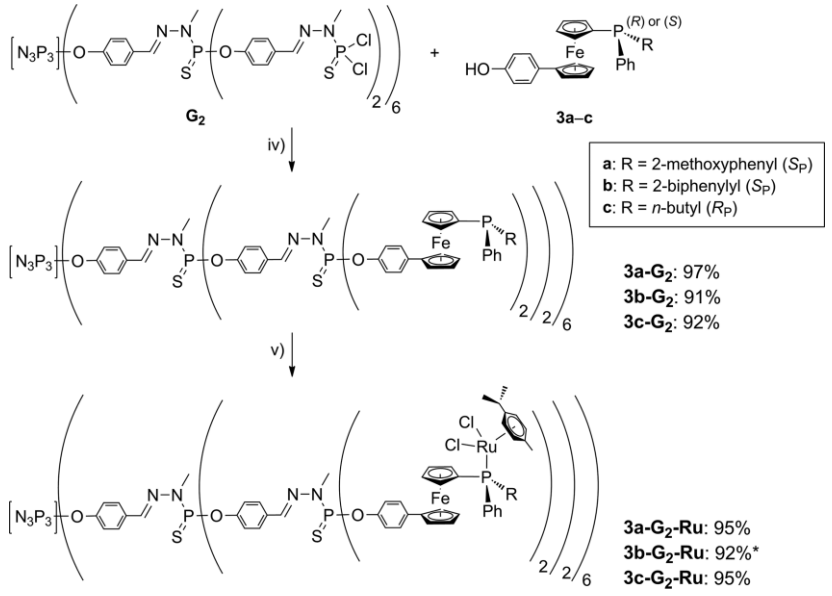

Scheme 4. Synthesis of the *P*-stereogenic dendritic ferrocenyl phosphine ruthenium complexes **3a–c-G_2-Ru**. iv) Cs_2CO_3, THF, r.t.; v) 12 equiv. [{Ru(*p*-cymene)Cl_2}$_2$], DCM, r.t. ***3b-G_2-Ru** forms a tethered complex with loss of the *p*-cymene ligand when activated by light.

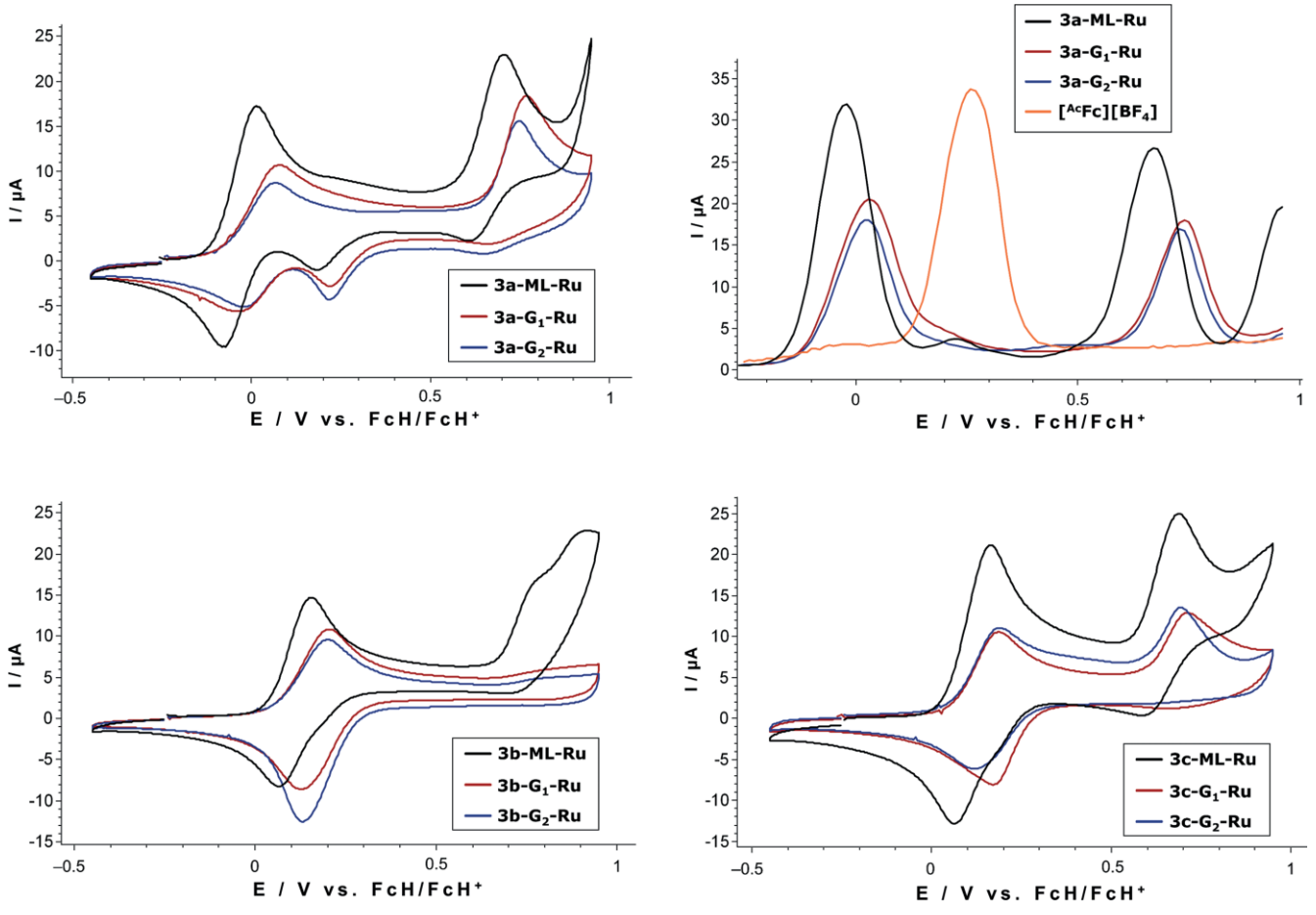

Figure 2. (Top left) Cyclic voltammetry of **3a-ML-Ru** and **3a-$G_{1,2}$-Ru**. (Top right) Square-wave voltammetry (positive mode) of **3a-ML-Ru**, **3a-$G_{1,2}$-Ru** and **[^{Ac}Fc][BF_4]**. (Bottom left) Cyclic voltammetry of **3b-ML-Ru** and **3b-$G_{1,2}$-Ru**. (Bottom right) Cyclic voltammetry of **3c-ML-Ru** and **3c-$G_{1,2}$-Ru**. 0.1 mol L^{-1} DCM/[$n$$Bu_4$N][$PF_6$], glassy carbon working electrode, referenced vs. ferrocene, scan rate = 100 mV s^{-1} ([^{Ac}Fc][BF_4] = acetylferrocenium tetrafluoroborate).

The cyclic voltammograms of all tested monomeric and dendritic ruthenium complexes exhibit a reversible one-electron redox process, which was assigned to Fe^{2+}/Fe^{3+}, with half-wave potentials between –0.03 V and 0.18 V (Table 1), whereby the potentials of the dendritic complexes are generally slightly higher than for the corresponding monomeric complexes. Furthermore, both first- and second-generation dendrimers behave electrochemically highly similar with only a single iron(II) redox wave, implying that all 12 (G_1) or 24 (G_2) ferrocene moieties are oxidized on the electrochemical timescale. In contrast to our previous studies on ferrocenyl phosphine ligands with aromatic spacers between ferrocene and phosphine,[64] all complexes tested here displayed an irreversible redox process for Ru^{2+}/Ru^{3+} with potentials between 0.64 V and 0.73 V (Table 1). Repeated electrochemical cycles (Figure 2 shows only the first scan of each measurement) showed decomposition of the complex after ruthenium(II) oxidation, which was further verified by observed adsorption processes on the electrode surface. However, cyclic voltammetry solely of the Fe^{2+}/Fe^{3+} redox process, with a forced vertex potential at 0.5 V, allowed repetitive electrochemical cycles without any signs of degradation showing the full reversibility of the iron(II) redox process as one essential requirement for desired redox-switched applications.

Table 1. Cyclic voltammetry data of the monomeric and dendritic complexes. 0.1 mol L^{-1} DCM/[nBu$_4$N][PF_6], glassy carbon working electrode, all half-wave potentials referenced vs. ferrocene, scan rate = 100 mV s^{-1}.

Entry	Compound	$E_{1/2}$ /V (Fe^{2+}/Fe^{3+})	$E_{1/2}$ /V (Ru^{2+}/Ru^{3+})
1	**3a-ML-Ru**	–0.03	0.66
2	**3b-ML-Ru**	0.11	0.73
3	**3c-ML-Ru**	0.11	0.64
4	**3a-G_1-Ru**	0.02	0.72
5	**3b-G_1-Ru**	0.16	–[a]
6	**3c-G_1-Ru**	0.18	0.68
7	**3a-G_2-Ru**	0.02	0.70
8	**3b-G_2-Ru**	0.17	–[a]
9	**3c-G_2-Ru**	0.15	0.67
10	**[^{Ac}Fc][BF_4]**	0.26	–
11	**[^{Ac2}fc][BF_4]**	0.49	–

[a] Distinct redox wave was not observed, no half-wave potential could be determined. [^{Ac}Fc][BF_4] = acetylferrocenium tetrafluoroborate, [^{Ac2}fc][BF_4] = diacetylferrocenium tetrafluoroborate.

Interestingly, the cyclic voltammograms of the 2-methoxyphenyl-substituted complexes **3a-ML-Ru** and **3a-$G_{1,2}$-Ru** showed an additional redox process with a potential at about 0.2 V (Figure 2, top left). This corresponds with our previous investigations on this complex showing its tendency for dimerization in solution at room temperature. A $RuCl_2$ fragment is coordinated by two ligand molecules **3a** in a chelating bidentate fashion via phosphorus and oxygen with complete displacement of the *p*-cymene ligand.[67] Consequently, this 2:1 (ligand/metal) complex exhibits two reversible one-electron redox processes at separated potentials reflecting two ferrocenyl moieties. Furthermore, the cyclic voltammograms of the 2-biphenylyl-substituted dendritic complexes **3b-$G_{1,2}$-Ru** showed no considerable redox process for ruthenium(II), as a consequence of the highly strained ruthenacycles formed by light-activated tethering (Figure 2, bottom left). Regarding the influence of different phosphorus substituents on the redox potential, the monomeric and dendritic complexes with 2-biphenylyl or *n*-butyl substituent exhibit similar iron(II) redox potentials in the cyclic voltammograms. Complexes with the electron-donating 2-methoxyphenyl substituent, in contrast, show lower iron(II) potentials being therefore easier to oxidize.

Among the oxidizing agents tested with regard to redox-switchable applications, acetylferrocenium tetrafluoroborate was the most suitable candidate since its oxidation potential of 0.26 V is highly suitable with respect to the electrochemical window (Figure 2, top right). Diacetylferrocenium tetrafluoroborate with an oxidation potential of 0.49 V, however, might partially interfere with the ruthenium redox process which would have detrimental effects on catalytic reactions. Classically, metal salts of silver(I) or copper(I) are commonly used as oxidizing agents,[72] which were not considered here in order to avoid catalyst poisoning.

Catalytic Tests

The monomeric and dendritic ruthenium(II) complexes were employed in the asymmetric transfer hydrogenation of acetophenone, which is the most utilized model substrate, dissolved in 2-propanol as hydrogen donor. Typically, catalytic precursors for this reaction are ruthenium(II) η^6-arene complexes with chiral polydentate nitrogen- or phosphorus-based ligands. Although less commonly applied, complexes of the type [$RuCl_2$(η^6-arene)P*] (P* = *P*-stereogenic monodentate phosphine) also feature catalytic activity and enantioselectivity in transfer hydrogenations.[56–59] These reactions are standardly performed in 2-propanol, acting as hydrogen donor and solvent at the same time, which opposes the unfavorable thermodynamics by shifting the equilibrium towards the desired product. Unfortunately, 2-propanol is a rather poor solvent for the dendritic complexes that we intended to apply in the hydrogen transfer reactions, thus requiring a suitable co-solvent. Dichloroethane (DCE) provided excellent solubility in combination with a boiling point high enough to be handled safely under catalytic conditions. Preliminary catalytic testing with different ratios of 2-propanol to DCE, however, showed erratic results with two major findings: The higher the percentage of DCE in 2-propanol, the lower the yield of the alcohol, and all reactions involving DCE did not show any noticeable enantioselectivity. Therefore, we turned our attention to different co-solvents with THF being the most suitable candidate due to excellent yield albeit low enantiomeric excess in the transfer hydrogenation of acetophenone (Table 2, entry 2). Additionally, we found that

Table 2. Effect of co-solvents on the transfer hydrogenation of acetophenone using **3a-ML-Ru**.[a]

Entry	Solvent (1:1)	yield (24 h) /%[b]	*ee* (24 h) /%
1	*i*PrOH/DCE	58	< 5
2	*i*PrOH/THF	95	15 (*S*)
3	*i*PrOH/$CHCl_3$	3	< 5
4	*i*PrOH/$C_6H_5CF_3$	37	< 5
5	*i*PrOH/1,4-dioxane	95	7 (*S*)
6	*i*PrOH/ethyl acetate	35	< 5

[a] Catalytic conditions (single runs): **3a-ML-Ru** (1.25 μmol) and *t*BuOK (12.5 μmol) dissolved in 1.6 mL of co-solvent and activated at 85 °C for 10 minutes before adding acetophenone (125.0 μmol in 1.6 mL of *i*PrOH). [b] Yields determined by GC-MS using anisole (125.0 μmol) as internal standard.

*i*PrOH:THF (1:1) gave similar results for catalytic activity and enantioselection as our tests with 100 % 2-propanol after 24 hours.

Further optimizations included the investigation of different bases in the transfer hydrogenation of acetophenone since the choice and amount of the base has a crucial influence on the outcome of the reaction. Among the most commonly used bases, we found that purified potassium *tert*-butoxide gave the highest yield of the alcohol after 24 hours reaction time (Table 3, entry 5). Another crucially important factor for obtaining reasonable conversions in these reactions is the activation period, in which the catalytic precursor is pre-heated in the presence of the base, generating the catalytically active ruthenium hydride species. This activation period is a highly sensitive process, and an optimal activation time of 15 minutes was reported for similar complexes.[57] However, we found that lowering the activation time from 15 to 10 minutes did not influence the catalytic reaction noticeably.

Table 3. Effect of base on the transfer hydrogenation of acetophenone using **3a-ML-Ru**.[a]

Entry	Base	yield (24 h) /%[b]
1	NaOH	28
2	KOH	47
3	Cs_2CO_3	52
4	*t*BuOK[c]	58
5	*t*BuOK[d]	63

[a] Catalytic conditions (single runs): **3a-ML-Ru** (1.25 μmol) and base (12.5 μmol) dissolved in 1.6 mL of DCE and activated at 85 °C for 10 minutes before adding acetophenone (125.0 μmol in 1.6 mL of *i*PrOH). [b] Yields determined by GC-MS using anisole (125.0 μmol) as internal standard. [c] Without purification. [d] Freshly purified by dissolving in dry THF, filtration and removal of solvent.

From a series of further pretrials, we concluded that the base is substantially necessary since performing the reaction without the addition of base hardly gave any alcohol after 24 hours. Furthermore, without ruthenium no conversion is observed, ensuring that the base itself is not catalytically active. In addition, we found that preformed precursors are considerably better catalysts than the ones formed in situ during the activation period from [{Ru(*p*-cymene)Cl_2}$_2$] and the corresponding ligand. Lastly, performing hydrogen transfers in the absence of the ferrocenyl phosphine ligands displayed only low to moderate yields under the same conditions.

Having established the best conditions to generate the catalytically active species, we performed catalytic runs with all synthesized monomeric (**3a–c-ML-Ru**) and dendritic (**3a–c-$G_{1,2}$-Ru**) complexes, using 1 mol-% ruthenium precursor and 10 mol-% potassium *tert*-butoxide (acetophenone/*t*BuOK/precursor = 100:10:1), in 2-propanol/THF (1:1) at 85 °C (Scheme 5). For comparison, we additionally used the structurally related achiral precursors with two phenyl substituents at phosphorus (**Ph-ML-Ru** and **Ph-$G_{1,2}$-Ru**, structures are given in the Supporting Information).[69] Since first- and second-generation dendrimers bear 12 (G_1) or 24 (G_2) catalytically active units per molecule, equal metal loadings had to be adhered throughout all catalytic reactions.

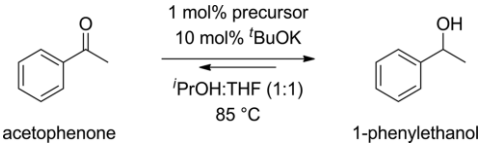

Scheme 5. Ruthenium-catalyzed transfer hydrogenation of acetophenone.

According to the performed test, all catalytic precursors are active in the transfer hydrogenation of acetophenone yielding 1-phenylethanol, which proceeded very cleanly since only acetophenone and its reduction product were detected by GC-MS. Furthermore, calibration to both reactant and product by using anisole as internal standard allowed determination of conversion and yield of every sample taken from the reaction. Thus, a selectivity of $S = 1$ was determined for all reactions, ensuring that converted reactant is entirely and solely used for yielding the product.

All monomeric complexes reached almost full conversion in the transfer hydrogenation of acetophenone after 24 hours (Table 4, entries 1–4), whereas all dendritic complexes performed worse than their monomeric analogs with yields between 41 % and 61 % after 24 hours (Table 4, entries 5–12). Interestingly, **Ph-G_1-Ru** and **Ph-G_2-Ru** displayed yields of 91 % and 85 % after 72 hours proving that the dendritic complexes successfully catalyze the hydrogen transfer but considerably slower than their monomeric analogs (Table 4, entries 5 and 9). However, the majority of reactions was terminated after 24 hours.

Table 4. Transfer hydrogenation of acetophenone catalyzed by **3a–c-ML-Ru**, **3a–c-G_1-Ru** and **3a–c-G_2-Ru**.[a]

Entry	Precursor	Time /h	Yield /%[b]	*ee* /%[c]
1	**Ph-ML-Ru**[69]	1/3/5/8/24	24/41/49/62/96	–
2	**3a-ML-Ru**	1/3/5/8/24	31/59/74/84/97	5 (*S*)
3	**3b-ML-Ru**	1/3/5/8/24	45/65/76/88/97	< 5
4	**3c-ML-Ru**	1/3/5/8/24	23/36/46/59/95	5 (*S*)
5	**Ph-G_1-Ru**[69]	1/3/5/8/24	9/21/28/41/53[d]	–
6	**3a-G_1-Ru**	1/3/5/8/24	6/14/22/33/58	8 (*S*)
7	**3b-G_1-Ru**	1/3/5/8/24	11/19/28/35/54	10 (*R*)
8	**3c-G_1-Ru**	1/3/5/8/24	8/15/20/29/54	< 5
9	**Ph-G_2-Ru**[69]	1/3/5/8/24	6/13/18/27/41[e]	–
10	**3a-G_2-Ru**	1/3/5/8/24	6/13/18/26/50	< 5
11	**3b-G_2-Ru**	1/3/5/8/24	9/19/27/33/61	6 (*R*)
12	**3c-G_2-Ru**	1/3/5/8/24	5/12/19/27/44	< 5

[a] Catalytic conditions (single runs): Precursor (1 mol-% Ru) dissolved in 6.5 mL of *t*BuOK (0.05 mmol in THF) and activated at 85 °C for 10 minutes before adding acetophenone (0.5 mmol in 6.5 mL of *i*PrOH). [b] Yields determined by GC-MS using anisole (0.5 mmol) as internal standard. [c] Enantiomeric excess at 24 h. [d] Yield after 72 h: 91 %. [e] Yield after 72 h: 85 %.

Regarding the dendrimer generations, it was found that the first-generation dendritic complexes **3a–c-G_1-Ru** are generally better precursors for the transfer hydrogenation of acetophenone than the second-generation dendritic complexes **3a–c-G_2-Ru** (Table 4, entries 5–8 and 9–12). Only **3b-G_2-Ru** displayed a slightly higher yield after 24 hours than its first-generation analog **3b-G_1-Ru** (61 % vs. 54 %). When comparing the influence of different phosphorus substituents on the catalytic performance, it is important to consider the formation of dimers of the monomeric 2-methoxyphenyl-substituted complex **3a-ML-Ru**,

Full Paper
doi.org/10.1002/ejic.202000142

as reported previously.[67] Therefore, it is highly likely that under catalytic conditions the formation of the described 2:1 (ligand/metal) complex is favored, in contrast to the initially synthesized 1:1 complex (Scheme 1). Generally, the 2-biphenylyl- and 2-methoxyphenyl-substituted complexes were more active catalysts in comparison to the *n*-butyl- and phenyl-substituted ones, which is particularly noticeable in case of the monomeric complexes **3a-ML-Ru** and **3b-ML-Ru** with very good yields of 84 % and 88 %, respectively, after eight hours already (Table 4, entries 2 and 3). For the 2-biphenylyl-substituted complexes, the strained structure generated by tethering might benefit the catalytic performance, as was previously observed for some tethered complexes when compared to untethered counterparts.[73]

In some of the transfer hydrogenation reactions using *P*-stereogenic ferrocenyl phosphine complexes, enantioenriched 1-phenylethanol was obtained but no explicit trends could be observed. **3b-G$_1$-Ru**, for instance, provided the *R* enantiomer of the alcohol with 10 % excess, the highest achieved along all tested precursors. In general, the 2-biphenylyl-substituted complexes seem to discriminate for the *R* form, whereas 2-methoxyphenyl- and *n*-butyl-substituted complexes afford preferably the *S* enantiomer. However, the overall enantioselection is very low for all precursors tested, as commonly found with similar monophosphine ligands;[56,73] some are even completely unselective, giving 1-phenylethanol with negligible enantiomeric excess (< 5 %). Thermal inversion at phosphorus under catalytic conditions was excluded, since previously reported inversion barriers for the monomeric complexes **3a–c-ML-Ru** indicated an estimated half-life of several days at 85 °C.[68] The enantioselectivity was only marginally better at low conversions, and lowering the temperature in general did not improve the enantioselection, but led to deficient conversions even for the monomeric precursors indicating slow deactivation over time.[74]

Redox-Switchable Catalysis

Leaving the unsatisfactory enantioselectivities aside, we combined the general catalytic properties with the electrochemical behavior of the monomeric and dendritic complexes and tested their suitability for redox-switchable catalysis. By chemical oxidation and subsequent reduction, the catalytic activity of the *P*-stereogenic monomeric and dendritic ferrocenyl phosphine complexes should be altered over the course of the hydrogen transfer reaction. However, second-generation dendritic complexes were not applied in redox-switched experiments since solubility limitations are generally becoming an issue going to higher generations, especially considering that in situ oxidation creates high positive charges.

On oxidation with acetylferrocenium tetrafluoroborate (1.0 equiv.) after 1.5 hours, the reaction rate for the monomeric complexes **3a–c-ML-Ru** was markedly reduced with the yields remaining at an almost constant level in the following hours (Figure 3, top). Only the achiral complex **Ph-ML-Ru** showed a slightly delayed response to the chemical oxidation. With reduction by decamethylferrocene (1.1 equiv.) after 5 hours, all monomeric complexes regained catalytic activity, albeit not on the same level as before oxidation. Although none of the redox-switched reactions reached the same yield as observed in the non-switched reactions, the influence of a redox-active ligand on the catalytic activity was remarkably demonstrated. The comparatively low yield in the reaction with **3c-ML-Ru** was due to overall poor catalytic performance even before oxidation.

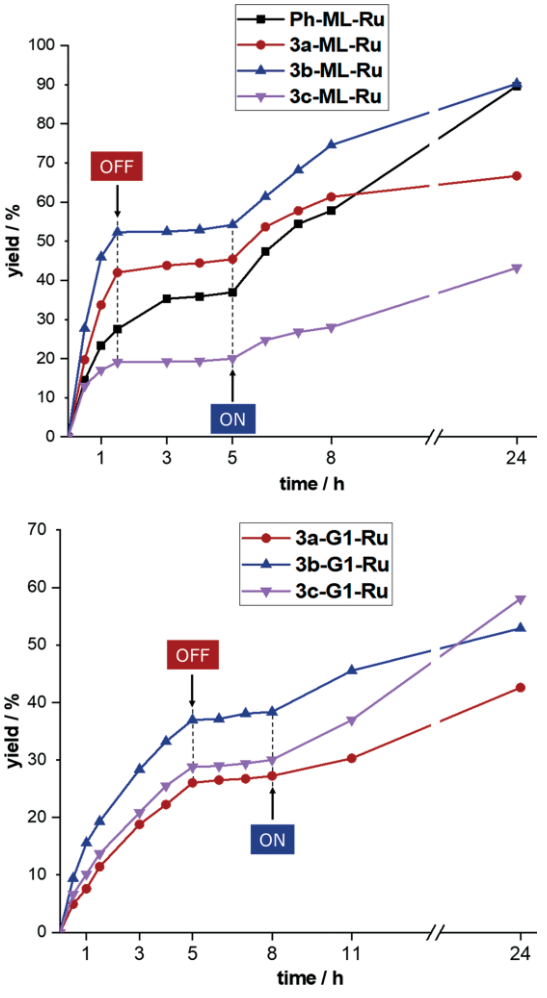

Figure 3. Redox-switched transfer hydrogenation of acetophenone catalyzed by monomeric complexes **Ph-ML-Ru** and **3a–c-ML-Ru** (top) and dendritic complexes **3a–c-G$_1$-Ru** (bottom) (OFF = 1.0 equiv. acetylferrocenium tetrafluoroborate, ON = 1.1 equiv. decamethylferrocene).

The same concept was applied to the dendritic complexes **3a–c-G$_1$-Ru** with different switching intervals to ensure a certain amount of conversion before oxidation was executed (Figure 3, bottom). All three dendritic complexes are less active catalysts upon oxidation after 5 hours, and subsequent reduction after 8 hours restored their catalytic activity. As we previously reported, oxidation might reduce the solubility of the dendritic complexes given the high positive charge.[65] Therefore, a potential solubility effect, in addition to the electronic communication, should not be excluded as explanation for a less active oxidized catalyst. However, the results of the monomeric catalysts in the redox-switched experiments clearly indicate an electronic effect of the redox-active ligand on the catalytic activity. Once the ferrocene is oxidized, iron(III) withdraws electron density from the phosphine decreasing its donor strength. Consequently, the electron-poor transition metal thus

created is a less active catalyst for the transfer hydrogenation of acetophenone. Therefore, reversible tuning of the electronic properties of the ruthenium catalyst in situ is possible.

The power of the concept of redox-switchable catalysis was furthermore proven by a double switching experiment performed with **3a-ML-Ru** by executing two oxidation and two reduction steps alternately (Figure 4). In comparison with previous catalytic runs, the complex still showed evident activity after the first oxidation which was endorsed by a separate experiment where the catalyst was oxidized in the activation period, revealing minor catalytic activity in the oxidized form. Furthermore, we demonstrated in a separate experiment that the reducing agent decamethylferrocene alone exhibited no catalytic activity, ascribing the regained catalytic activity after reduction exclusively to the catalyst.

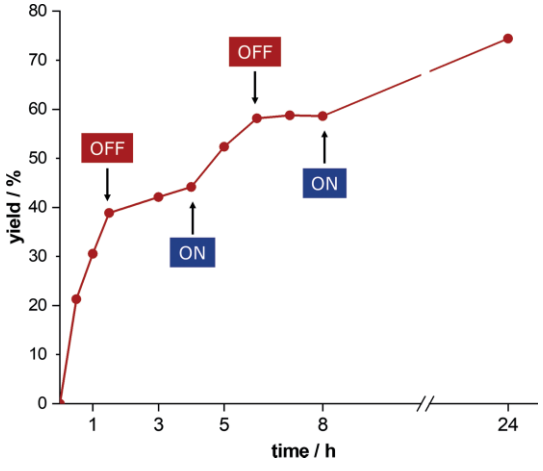

Figure 4. Redox-switched transfer hydrogenation of acetophenone catalyzed by **3a-ML-Ru** with two switching events (OFF = 1.0 equiv. acetylferrocenium tetrafluoroborate, ON = 1.1 equiv. decamethylferrocene).

Conclusion

A new homogeneous catalytic system for the redox-switchable asymmetric transfer hydrogenation of acetophenone has been developed and, consequently, the first application of phosphine ligands in redox-switchable transfer hydrogenation catalysis was achieved. *P*-stereogenic phosphines were coupled to a redox-active ferrocene moiety which was furthermore utilized to immobilize this ligand system on phosphorus-containing dendrimers. Ruthenium(II) complexes of these *P*-stereogenic dendritic ferrocenyl phosphines and their monomeric counterparts were electrochemically characterized proving their suitability for redox-switchable applications. Catalytic testing of these complexes revealed general catalytic activity for the transfer hydrogenation with moderate (dendritic complexes) to excellent (monomeric complexes) yields after 24 hours reaction time. The first-generation dendrimers were more active than the second-generation dendrimers; thus, no positive dendritic effect could be observed. Overall unsatisfactory enantioselection afforded an enantioenriched reduction product in only some cases. By utilizing the electrochemical properties, the concept of redox-switchable catalysis was applied, and the catalytic activity of the complexes was altered over the course of the hydrogen transfer reaction. Both monomeric and dendritic complexes are switchable catalysts with markedly decreased catalytic activity in the oxidized form. In situ reduction restored the catalytic activity, although to a lesser extent than before oxidation.

These results expand the use of redox-active phosphine ligands in redox-switchable catalysis. Especially transfer hydrogenations, as a powerful alternative for direct hydrogenations, have been scarcely explored in combination with redox-switchable catalysts. Redox control, in general, not only enables an enhanced understanding of catalytic mechanisms but also facilitates the development towards catalysts with orthogonal activity for different substrates depending on their redox state. Additionally, dendritic catalysts might contribute to this development by addressing the limited recyclability of homogeneous catalysts. Future improvement of the ligand system presented here should involve the introduction of *P*-stereogenic bisphosphines aiming for enhanced stereodiscrimination and, therefore, improved enantioselectivities in the asymmetric catalytic transformations.

Experimental Section

General Procedure and Analytical Methods

In case of moisture or air sensitivity, the reactions were conducted under nitrogen atmosphere using Schlenk techniques. Diethyl ether, dichloromethane, toluene and hexane (isomeric mixture) were obtained from an MBraun Solvent Purification System SPS-800 and stored over 4 Å molecular sieves or potassium (in case of hexane). THF was dried and distilled from potassium, diethylamine was dried and distilled from potassium hydroxide. The starting material 1-bromo-1′-[(4-phenoxy)*tert*-butyldimethylsilyl]-ferrocene[65,69] was synthesized from 1,1′-dibromoferrocene[75] according to literature procedures. The methyl (phenyl)phosphinite boranes[70] were synthesized by way of an (–)-ephedrine-based oxazaphospholidine borane complex. The dendrimers $\mathbf{G_1}$ and $\mathbf{G_2}$,[71] and acetylferrocenium tetrafluoroborate[72] were synthesized according to literature procedures. Acetophenone and anisole were freshly distilled, *t*BuOK freshly purified and decamethylferrocene freshly sublimed prior use. Di-μ-chlorobis[(η^6-*p*-cymene)chlororuthenium(II)] is commercially available and was used without further purification. NMR spectra were recorded with a Bruker Avance III HD 400 or Bruker Ascend 400 spectrometer. Numbering schemes for the assignment of NMR signals are included in the Supporting Information. Mass spectra were obtained with a Bruker ESI-TOF micrOTOF, a Bruker ESI-qTOF Impact II and a Bruker Esquire 3000plus spectrometer. Elemental analyses were determined with a Heraeus Vario EL Analyser. IR spectra were obtained with a Perkin-Elmer FT-IR Spectrum 2000 spectrometer. The samples were measured as KBr pellets. Chiral HPLC was performed with a Knauer HPLC system with a Smartline PDA 2800 detector (λ = 233 nm) and a 250 × 4.6 mm Lux® 5 μm Amylose-1 column by Phenomenex. The specific rotations were measured with a Krüss Optronic P3002RS automatic digital polarimeter using a 1 dm micro polarimeter tube from Schmidt + Haensch. Melting points were determined using a Gallenkamp MPD 350 BM 2.5 capillary melting point apparatus and are reported uncorrected. All electrochemical measurements were obtained at room temperature with a Biologic Science Instruments SP-50 potentiostat using a three-electrode cell setup from Gamry Instruments

(glassy carbon working electrode, platinum counter electrode and non-aqueous Ag/Ag^+ reference electrode) with 0.1 mol L^{-1} [nBu$_4$N][PF_6] in DCM as electrolyte. GC analyses were performed with a GC-MS system GC-MS-QP2010 from Shimadzu with helium as carrier gas. All samples were analyzed by using a 30 m × 0.25 mm β-DEX™ 120 chiral capillary column by Supelco with anisole as internal standard. Enantiomers were assigned by comparison with commercially available enantiopure compounds. X-ray diffraction studies were performed with an Oxford Diffraction CCD Xcalibur-S diffractometer using Mo-K_α radiation and ω-scan rotation. All dendritic compounds were characterized exclusively by NMR spectroscopy since dendrimers are known for solvent inclusions falsifying other characterization results.

Synthesis of Silyl-Protected Ferrocenyl Phosphine Boranes 1a–c

At –80 °C, *n*BuLi in hexanes (1.10 equiv.) was slowly added to a solution of 1-bromo-1′-[(4-phenoxy)*tert*-butyldimethylsilyl]ferrocene (1.05 equiv.) in THF (0.25 mol L^{-1}). After stirring for 1 h at –80 °C, the reaction mixture was slowly added to a solution of the corresponding methyl (phenyl)phosphinite borane (1.00 equiv.) in THF (0.25 mol L^{-1}) at –80 °C. The solution was warmed to room temperature over a period of 12 h. Water was added and the aqueous phase was extracted with diethyl ether. The combined organic layers were washed with saturated aqueous NaCl and dried with $MgSO_4$. After removal of the solvent in vacuo, the crude product was purified by column chromatography on silica with hexane/DCM (4:1) grad. hexane/DCM (1:1).

1-[(S_P)-(2-Methoxyphenyl)(phenyl)phosphine *P*-borane]-1′-[(4-phenoxy)*tert*-butyldimethylsilyl]ferrocene (1a). Ferrocenyl phosphine borane **1a** was obtained from methyl (R_P)-(2-methoxyphenyl)(phenyl)phosphinite *P*-borane (0.68 g, 2.63 mmol) as a sticky orange solid (0.85 g, 52 %). Its enantiomeric excess was determined by analytical chiral HPLC (hexane/2-propanol 90:10, 0.5 mL min^{-1}): *ee* = 97.5 % (t_R: 10.0 min [S_P], 10.7 min [R_P]). R_f: 0.27 (hexane/DCM, 2:1, v/v). mp: 66–68 °C. $[\alpha]_D^{25}$ = –18.3 (*c* = 1.25, $CHCl_3$). ^{1}H-NMR (400.2 MHz, $CDCl_3$): δ (ppm) = 0.20 (s, 6H, H28), 0.73–1.82 (br m, 3H, BH_3), 0.99 (s, 9H, H26), 3.41 (s, 3H, H25), 4.14–4.16 (m, 1H, H7/8), 4.16–4.18 (m, 1H, H7/8), 4.26–4.28 (m, 1H, H11/12), 4.28–4.30 (m, 1H, H11/12), 4.38–4.39 (m, 1H, H6/H9), 4.40–4.41 (m, 1H, H10/13), 4.42–4.43 (m, 1H, H10/13), 4.45–4.46 (m, 1H, H6/H9), 6.67 (d, 2H, $^3J_{HH}$ = 8.6 Hz, H3), 6.84–6.87 (m, 1H, H23), 7.06 (d, 2H, $^3J_{HH}$ = 8.6 Hz, H2), 7.07–7.12 (m, 1H, H21), 7.30–7.40 (m, 3H, H17, H18), 7.46–7.53 (m, 3H, H16, H22), 7.84–7.90 (m, 1H, H20). ^{13}C{^{1}H}-NMR (100.6 MHz, $CDCl_3$): δ (ppm) = –4.2 (s, C28), 18.4 (s, C27), 25.8 (s, C26), 55.3 (s, C25), 67.3 (s, C6/C9), 67.5 (s, C6/C9), 69.0 (d, $^1J_{CP}$ = 70.1 Hz, C14), 71.0 (s, C7/C8), 71.0 (s, C7/C8), 73.8 (d, $^3J_{CP}$ = 8.3 Hz, C11/12), 74.1 (d, $^3J_{CP}$ = 7.5 Hz, C11/12), 75.0 (d, $^2J_{CP}$ = 13.9 Hz, C10/C13), 75.1 (d, $^2J_{CP}$ = 8.2 Hz, C10/C13), 87.0 (s, C5), 112.0 (d, $^3J_{CP}$ = 4.2 Hz, C23), 119.7 (d, $^1J_{CP}$ = 58.1 Hz, C19), 120.1 (s, C3), 121.1 (d, $^3J_{CP}$ = 11.7 Hz, C21), 127.1 (s, C2), 128.0 (d, $^3J_{CP}$ = 10.5 Hz, C17), 130.0 (d, $^4J_{CP}$ = 2.2 Hz, C18), 130.6 (s, C4), 131.5 (d, $^2J_{CP}$ = 10.0 Hz, C16), 132.8 (d, $^1J_{CP}$ = 62.7 Hz, C15), 133.5 (d, $^4J_{CP}$ = 1.4 Hz, C22), 135.8 (d, $^2J_{CP}$ = 12.8 Hz, C20), 154.3 (s, C1), 161.0 (s, C24). ^{31}P{^{1}H}-NMR (162.0 MHz, $CDCl_3$): δ (ppm) = 13.7 (br m). ESI(+)-MS: *m/z* (%) = 643.2 (98.0) $[M + Na]^+$, 620.2 (100) $[M]^+$, 607.2 (26.1) $[M – BH_3]^+$. FT-IR (KBr): $\tilde{\nu}$ (cm^{-1}) = 3444 m, 3062 w, 2954 m, 2930 m, 2887 m, 2856 m, 2381 m, 2257 w, 1607 m, 1589 m, 1574 m, 1524 s, 1476 s, 1458 s, 1433 m, 1389 w, 1362 w, 1254 s, 1169 m, 1134 w, 1104 w, 1059 m, 1027 m, 913 s, 836 s, 804 m, 781 m, 758 m, 742 m, 697 m, 673 w, 634 w, 610 w, 582 w, 529 m, 499 m. Anal. Calcd. for $C_{35}H_{42}BFeO_2PSi$ (620.2): C 67.76, H 6.82; found C 67.33, H 6.73.

1-[(S_P)-(2-Biphenylyl)(phenyl)phosphine *P*-borane]-1′-[(4-phenoxy)*tert*-butyl-dimethylsilyl]ferrocene (1b). Ferrocenyl phosphine borane **1b** was obtained from methyl (R_P)-(2-biphenylyl)(phenyl)-phosphinite *P*-borane (0.20 g, 0.65 mmol) as an orange solid (0.22 g, 51 %). Its enantiomeric excess was determined by analytical chiral HPLC (hexane/2-propanol 90:10, 0.25 mL min^{-1}): *ee* = 97.1 % (t_R: 17.3 min [S_P], 18.1 min [R_P]). R_f: 0.30 (hexane/DCM, 2:1, v/v). mp: 57–59 °C. $[\alpha]_D^{25}$ = –13.8 (*c* = 1.25, $CHCl_3$). ^{1}H-NMR (400.2 MHz, $CDCl_3$): δ (ppm) = 0.19 (s, 6H, H31), 0.65–1.66 (br m, 3H, BH_3), 0.98 (s, 9H, H29), 3.85–3.86 (m, 1H, H7/8), 3.88–3.89 (m, 1H, H11/12), 4.01–4.03 (m, 2H, H6/H9, H7/H8), 4.16–4.17 (m, 1H, H11/12), 4.20–4.22 (m, 1H, H10/13), 4.53–4.54 (m, 1H, H6/H9), 4.58–4.60 (m, 1H, H10/13), 6.66 (d, 2H, $^3J_{HH}$ = 8.6 Hz, H3), 6.87 (br s, 2H, H27), 6.99 (t, 2H, $^3J_{HH}$ = 7.5 Hz, H26), 7.02–7.14 (m, 2H, H23, H28), 7.04 (d, 2H, $^3J_{HH}$ = 8.7 Hz, H2), 7.20–7.26 (m, 2H, H20, H21), 7.32–7.40 (m, 3H, H17, H18), 7.43–7.48 (m, 1H, H22), 7.57–7.62 (m, 2H, H16). ^{13}C{^{1}H}-NMR (100.6 MHz, $CDCl_3$): δ (ppm) = –4.2 (s, C31), 18.4 (s, C30), 25.8 (s, C29), 67.2 (s, C6/C9), 67.5 (s, C6/C9), 71.2 (s, C7/C8), 71.4 (s, C7/C8), 71.6 (d, $^1J_{CP}$ = 68.8 Hz, C14), 72.7 (d, $^3J_{CP}$ = 1.8 Hz, C11/12), 74.3 (d, $^2J_{CP}$ = 8.9 Hz, C10/C13), 74.5 (d, $^3J_{CP}$ = 6.2 Hz, C11/C12), 76.2 (d, $^2J_{CP}$ = 16.4 Hz, C10/C13), 87.1 (s, C5), 120.1 (s, C3), 126.9 (d, $^2J_{CP}$ = 9.2 Hz, C20), 127.0 (s, C28), 127.1 (s, C2), 127.1 (s, C26), 128.3 (d, $^3J_{CP}$ = 10.3 Hz, C17), 130.1 (d, $^4J_{CP}$ = 1.6 Hz, C18), 130.2 (s, C27), 130.5 (s, C4), 131.0 (d, $^4J_{CP}$ = 2.5 Hz, C22), 131.4 (d, $^1J_{CP}$ = 31.3 Hz, C15), 131.8 (s, C25), 131.9 (d, $^3J_{CP}$ = 7.9 Hz, C23), 133.2 (d, $^2J_{CP}$ = 9.5 Hz, C16), 133.6 (d, $^3J_{CP}$ = 8.8 Hz, C21), 140.5 (d, $^2J_{CP}$ = 3.1 Hz, C24), 146.8 (d, $^1J_{CP}$ = 9.5 Hz, C19), 154.3 (s, C1). ^{31}P{^{1}H}-NMR (162.0 MHz, $CDCl_3$): δ (ppm) = 17.8 (br m). ESI(+)-MS: *m/z* (%) = 689.2 (63.2) $[M + Na]^+$, 653.2 (100) $[M – BH_3]^+$. FT-IR (KBr): $\tilde{\nu}$ (cm^{-1}) = 3441 m, 3054 w, 2928 m, 2856 m, 2371 m, 1607 m, 1561 w, 1524 s, 1457 s, 1438 m, 1389 w, 1263 s, 1169 m, 1103 w, 1057 m, 1028 m, 913 s, 829 s, 805 m, 780 m, 743 m, 697 m, 668 m, 606 w, 528 w, 496 w. Anal. Calcd. for $C_{40}H_{44}BFeOPSi$ (666.2): C 72.08, H 6.65; found C 72.46, H 6.80.

1-[(R_P)-(*n*-Butyl)(phenyl)phosphine *P*-borane]-1′-[(4-phenoxy)-*tert*-butyl-dimethylsilyl]ferrocene (1c). Ferrocenyl phosphine borane **1c** was obtained from methyl (S_P)-(*n*-butyl)(phenyl)-phosphinite *P*-borane (0.80 g, 3.81 mmol) as an orange oil (1.11 g, 51 %). Its enantiomeric excess was determined by analytical chiral HPLC (hexane/2-propanol 90:10, 0.5 mL min^{-1}): *ee* = 98.1 % (t_R: 6.6 min [S_P], 8.3 min [R_P]). R_f: 0.23 (hexane/DCM, 2:1, v/v). $[\alpha]_D^{25}$ = +54.7 (*c* = 1.25, $CHCl_3$). ^{1}H-NMR (400.2 MHz, $CDCl_3$): δ (ppm) = 0.21 (s, 6H, H25), 0.55–1.78 (br m, 3H, BH_3), 0.99 (s, 9H, H23), 0.83–0.90 (m, 3H, H22), 1.26–1.34 (m, 2H, H21), 1.50–1.58 (m, 2H, H20), 1.93–2.00 (m, 2H, H19), 4.18–4.19 (m, 2H, H10/H13, H11/H12), 4.25–4.27 (m, 2H, H7/H8, H10/H13), 4.29–4.30 (m, 1H, H7/H8), 4.33–4.35 (m, 1H, H11/H12), 4.48–4.49 (m, 1H, H6/H9), 4.65–4.67 (m, 1H, H6/H9), 6.73 (d, 2H, $^3J_{HH}$ = 8.5 Hz, H3), 7.23 (d, 2H, $^3J_{HH}$ = 8.5 Hz, H2), 7.42–7.50 (m, 3H, H17, H18), 7.72–7.77 (m, 2H, H16). ^{13}C{^{1}H}-NMR (100.6 MHz, $CDCl_3$): δ (ppm) = –4.2 (s, C25), 13.7 (s, C22), 18.4 (s, C24), 24.4 (d, $^2J_{CP}$ = 14.4 Hz, C20), 25.4 (s, C21), 25.8 (s, C23), 27.6 (d, $^1J_{CP}$ = 38.9 Hz, C19), 67.5 (s, C6/C9), 67.5 (s, C6/C9), 70.8 (s, C7/C8), 70.8 (s, C7/C8), 71.0 (d, $^1J_{CP}$ = 65.0 Hz, C14), 72.9 (d, $^3J_{CP}$ = 9.5 Hz, C11/12), 73.1 (d, $^3J_{CP}$ = 9.7 Hz, C11/12), 73.6 (d, $^2J_{CP}$ = 7.4 Hz, C10/C13), 74.0 (d, $^2J_{CP}$ = 7.4 Hz, C10/C13), 87.2 (s, C5), 120.2 (s, C3), 127.3 (s, C2), 128.6 (d, $^3J_{CP}$ = 9.7 Hz, C17), 130.5 (d, $^1J_{CP}$ = 54.9 Hz, C15), 130.0 (s, C4), 131.1 (d, $^4J_{CP}$ = 1.9 Hz, C18), 132.2 (d, $^2J_{CP}$ = 8.9 Hz, C16), 154.5 (s, C1). ^{31}P{^{1}H}-NMR (162.0 MHz, $CDCl_3$): δ (ppm) = 11.2 (br m). ESI(+)-MS: *m/z* (%) = 593.2 (33.9) $[M + Na]^+$, 570.2 (100) $[M]^+$. FT-IR (KBr): $\tilde{\nu}$ (cm^{-1}) = 3438 m, 3059 w, 3032 w, 2958 m, 2930 m, 2899 w, 2858 m, 2381 m, 2344 m, 2254 w, 1608 m, 1525 s, 1458 s, 1437 w, 1413 w, 1387 w, 1362 w, 1261 s, 1172 m, 1105 m, 1066 m, 1030 m, 913 s, 828 s, 805 s, 783 m, 741 m, 697 m, 672 w, 630 w, 601 w, 529 m, 495 m. HR-MS [ESI(+)]: *m/z* $[M]^+$ calcd. for $C_{32}H_{44}BFeOPSi$: 570.2343; found 570.2355.

Synthesis of Ferrocenyl Phosphine Boranes 2a–c

Tetra-*n*-butylammonium fluoride trihydrate (2.00 equiv.) was added to a solution of **1a**–**c** (1.00 equiv.) in THF (0.02 mol L^{-1}) and stirred for 12 h at room temperature. Ethyl acetate was added and the organic phase was washed with saturated aqueous NH_4Cl and dried with $MgSO_4$. After removal of the solvent in vacuo, the crude product was purified by column chromatography on silica with hexane/DCM, 1:1 grad. DCM.

1-[(S_P)-(2-Methoxyphenyl)(phenyl)phosphine *P*-borane]-1′-(4-hydroxyphenyl)ferrocene (2a). Ferrocenyl phosphine borane **2a** was obtained from silyl-protected ferrocenyl phosphine borane **1a** (0.50 g, 0.81 mmol) as an orange solid (0.38 g, 93 %). Its enantiomeric excess was determined by analytical chiral HPLC (hexane/2-propanol 85:15, 0.5 mL min^{-1}): *ee* = 96.6 % (t_R: 33.8 min [S_P], 36.3 min [R_P]). R_f: 0.16 (hexane/DCM, 1:2, v/v). mp: 113–115 °C. $[\alpha]_D^{25}$ = –20.3 (*c* = 1.25, $CHCl_3$). ^{1}H-NMR (400.2 MHz, $CDCl_3$): δ (ppm) = 0.68–1.77 (br m, 3H, BH_3), 3.40 (s, 3H, H25), 4.14–4.15 (m, 1H, H7/8), 4.16–4.17 (m, 1H, H7/8), 4.28–4.29 (m, 1H, H11/12), 4.31–4.32 (m, 1H, H11/12), 4.39–4.40 (m, 2H, H6/H9, H10/13), 4.41–4.42 (m, 1H, H10/13), 4.45–4.46 (m, 1H, H6/9), 4.77 (br s, 1H, OH), 6.67 (d, 2H, $^3J_{HH}$ = 8.5 Hz, H3), 6.84–6.87 (m, 1H, H23), 7.06 (d, 2H, $^3J_{HH}$ = 8.6 Hz, H2), 7.07–7.12 (m, 1H, H21), 7.30–7.40 (m, 3H, H17, H18), 7.46–7.53 (m, 3H, H16, H22), 7.84–7.89 (m, 1H, H20). ^{13}C{^{1}H}-NMR (100.6 MHz, $CDCl_3$): δ (ppm) = 55.3 (s, C25), 67.3 (s, C6/C9), 67.5 (s, C6/C9), 69.0 (d, $^1J_{CP}$ = 70.2 Hz, C14), 70.9 (s, C7/C8), 70.9 (s, C7/C8), 73.7 (d, $^3J_{CP}$ = 8.3 Hz, C11/12), 74.0 (d, $^3J_{CP}$ = 7.5 Hz, C11/12), 75.0 (d, $^2J_{CP}$ = 12.6 Hz, C10/C13), 75.2 (d, $^2J_{CP}$ = 7.8 Hz, C10/C13), 87.1 (s, C5), 112.0 (d, $^3J_{CP}$ = 4.3 Hz, C23), 115.4 (s, C3), 119.6 (d, $^1J_{CP}$ = 58.3 Hz, C19), 121.1 (d, $^3J_{CP}$ = 11.7 Hz, C21), 127.4 (s, C2), 128.0 (d, $^3J_{CP}$ = 10.5 Hz, C17), 130.0 (d, $^4J_{CP}$ = 2.1 Hz, C18), 130.2 (s, C4), 131.4 (d, $^2J_{CP}$ = 10.0 Hz, C16), 132.7 (d, $^1J_{CP}$ = 62.7 Hz, C15), 133.6 (d, $^4J_{CP}$ = 1.4 Hz, C22), 135.7 (d, $^2J_{CP}$ = 12.8 Hz, C20), 154.2 (s, C1), 161.0 (s, C24). ^{31}P{^{1}H}-NMR (162.0 MHz, $CDCl_3$): δ (ppm) = 13.7 (br m). ESI(+)-MS: *m*/*z* (%) = 529.1 (89.8) $[M + Na]^+$, 515.1 (100) $[M – BH_3 + Na]^+$, 492.1 (98.3) $[M – BH_3]^+$. FT-IR (KBr): $\tilde{\nu}$ (cm^{-1}) = 3922 w, 3430 s, 3136 w, 3105 w, 3062 w, 3036 w, 3010 w, 2966 w, 2939 w, 2836 w, 2378 s, 2366 s, 2299 m, 2270 m, 1956 w, 1910 w, 1887 w, 1799 w, 1769 w, 1704 w, 1675 w, 1647 w, 1610 m, 1588 m, 1526 s, 1478 s, 1456 s, 1433 s, 1388 w, 1348 m, 1325 w, 1301 w, 1278 s, 1264 s, 1250 s, 1213 s, 1193 s, 1169 s, 1138 m, 1106 m, 1068 s, 1029 s, 1013 m, 890 w, 834 s, 808 m, 756 s, 726 m, 702 m, 689 m, 655 w, 636 m, 614 m, 584 w, 531 m, 509 s, 496 s, 461 s, 428 w. Anal. Calcd. for $C_{29}H_{28}BFeO_2P$ (506.1): C 68.81, H 5.58; found C 68.75, H 5.56.

1-[(S_P)-(2-Biphenylyl)(phenyl)phosphine *P*-borane]-1′-(4-hydroxyphenyl)ferrocene (2b). Ferrocenyl phosphine borane **2b** was obtained from silyl-protected ferrocenyl phosphine borane **1b** (0.62 g, 0.92 mmol) as an orange solid (0.38 g, 75 %). Its enantiomeric excess was determined by analytical chiral HPLC (hexane/2-propanol 85:15, 0.5 mL min^{-1}): *ee* = 96.3 % (t_R: 27.9 min [S_P], 42.3 min [R_P]). R_f: 0.19 (hexane/DCM, 1:2, v/v). mp: 96–98 °C. $[\alpha]_D^{25}$ = +19.7 (*c* = 1.25, $CHCl_3$). ^{1}H-NMR (400.2 MHz, $CDCl_3$): δ (ppm) = 0.61–1.64 (br m, 3H, BH_3), 3.86–3.88 (m, 1H, H7/8), 3.88–3.89 (m, 1H, H11/12), 3.99–4.00 (m, 1H, H7/H8), 4.03–4.05 (m, 1H, H6/H9), 4.19–4.20 (m, 1H, H11/12), 4.22–4.24 (m, 1H, H10/13), 4.52–4.53 (m, 1H, H6/H9), 4.57–4.59 (m, 1H, H10/13), 4.67 (br s, 1H, OH), 6.66 (d, 2H, $^3J_{HH}$ = 8.6 Hz, H3), 6.87 (br s, 2H, H27), 6.99 (t, 2H, $^3J_{HH}$ = 7.5 Hz, H26), 7.03–7.14 (m, 2H, H23, H28), 7.05 (d, 2H, $^3J_{HH}$ = 8.6 Hz, H2), 7.17–7.25 (m, 2H, H20, H21), 7.33–7.40 (m, 3H, H17, H18), 7.44–7.48 (m, 1H, H22), 7.57–7.62 (m, 2H, H16). ^{13}C{^{1}H}-NMR (100.6 MHz, $CDCl_3$): δ (ppm) = 67.2 (s, C6/C9), 67.5 (s, C6/C9), 71.1 (s, C7/C8), 71.3 (s, C7/C8), 71.7 (d, $^1J_{CP}$ = 68.4 Hz, C14), 72.7 (d, $^3J_{CP}$ = 2.0 Hz, C11/12), 74.2 (d, $^2J_{CP}$ = 8.9 Hz, C10/C13), 74.4 (d, $^3J_{CP}$ = 6.2 Hz, C11/C12), 76.3 (d, $^2J_{CP}$ = 16.5 Hz, C10/C13), 87.0 (s, C5), 115.4 (s, C3), 126.9 (d, $^2J_{CP}$ = 9.2 Hz, C20), 127.1 (s, C28), 127.1 (s, C2), 127.4 (s, C26), 128.3 (d, $^3J_{CP}$ = 10.3 Hz, C17), 130.1 (d, $^4J_{CP}$ = 1.9 Hz, C18), 130.2 (s, C27), 131.0 (s, C4), 131.0 (d, $^4J_{CP}$ = 2.3 Hz, C22), 131.4 (d, $^1J_{CP}$ = 34.3 Hz, C15), 131.8 (s, C25), 131.9 (d, $^3J_{CP}$ = 7.9 Hz, C23), 133.3 (d, $^2J_{CP}$ = 9.5 Hz, C16), 133.6 (d, $^3J_{CP}$ = 8.7 Hz, C21), 140.5 (d, $^2J_{CP}$ = 3.3 Hz, C24), 146.9 (d, $^1J_{CP}$ = 9.6 Hz, C19), 154.2 (s, C1). ^{31}P{^{1}H}-NMR (162.0 MHz, $CDCl_3$): δ (ppm) = 17.8 (br m). ESI(+)-MS: *m*/*z* (%) = 552.1 (18.0) $[M]^+$, 538.1 (100) $[M – BH_3]^+$. FT-IR (KBr): $\tilde{\nu}$ (cm^{-1}) = 3924 w, 3775 w, 3716 w, 3689 w, 3419 s, 3053 m, 2955 m, 2384 s, 2361 m, 1734 w, 1687 w, 1651 w, 1647 w, 1611 m, 1562 w, 1556 w, 1540 w, 1527 s, 1497 w, 1458 m, 1438 s, 1385 m, 1363 w, 1264 m, 1215 m, 1170 s, 1106 m, 1085 w, 1058 m, 1030 m, 1008 w, 886 w, 830 s, 745 s, 699 s, 668 m, 634 w, 608 w, 530 w, 498 m, 469 m, 421 w. Anal. Calcd. for $C_{34}H_{30}BFeOP$ (552.2): C 72.95, H 5.48; found C 72.65, H 5.78.

1-[(R_P)-(*n*-Butyl)(phenyl)phosphine *P*-borane]-1′-(4-hydroxyphenyl)ferrocene (2c). Ferrocenyl phosphine borane **2c** was obtained from silyl-protected ferrocenyl phosphine borane **1c** (0.92 g, 1.62 mmol) as a sticky orange solid (0.66 g, 89 %). Its enantiomeric excess was determined by analytical chiral HPLC (hexane/2-propanol 85:15, 0.5 mL min^{-1}): *ee* = 94.6 % (t_R: 19.0 min [R_P], 20.4 min [S_P]). R_f: 0.19 (hexane/DCM, 1:2, v/v). $[\alpha]_D^{25}$ = +69.7 (*c* = 1.25, $CHCl_3$). ^{1}H-NMR (400.2 MHz, $CDCl_3$): δ (ppm) = 0.51–1.65 (br m, 3H, BH_3), 0.82–0.86 (m, 3H, H22), 1.24–1.34 (m, 2H, H21), 1.49–1.56 (m, 2H, H20), 1.89–2.02 (m, 2H, H19), 4.17–4.19 (m, 1H, H11/H12), 4.19–4.20 (m, 1H, H10/H13), 4.26–4.27 (m, 1H, H7/H8), 4.28–4.29 (m, 2H, H7/H8, H10/H13), 4.34–4.35 (m, 1H, H11/H12), 4.48–4.49 (m, 1H, H6/H9), 4.65–4.66 (m, 1H, H6/H9), 4.99 (br s, 1H, OH), 6.75 (d, 2H, $^3J_{HH}$ = 8.5 Hz, H3), 7.24 (d, 2H, $^3J_{HH}$ = 8.5 Hz, H2), 7.41–7.50 (m, 3H, H17, H18), 7.73–7.77 (m, 2H, H16). ^{13}C{^{1}H}-NMR (100.6 MHz, $CDCl_3$): δ (ppm) = 13.7 (s, C22), 24.3 (d, $^2J_{CP}$ = 14.4 Hz, C20), 25.4 (s, C21), 27.6 (d, $^1J_{CP}$ = 39.0 Hz, C19), 67.4 (s, C6/C9), 67.5 (s, C6/C9), 70.7 (s, C7/C8), 70.8 (s, C7/C8), 70.9 (d, $^1J_{CP}$ = 65.1 Hz, C14), 72.9 (d, $^3J_{CP}$ = 9.4 Hz, C11/12), 73.1 (d, $^3J_{CP}$ = 9.8 Hz, C11/12), 73.5 (d, $^2J_{CP}$ = 7.4 Hz, C10/C13), 73.9 (d, $^2J_{CP}$ = 7.4 Hz, C10/C13), 87.2 (s, C5), 115.5 (s, C3), 127.5 (s, C2), 128.7 (d, $^3J_{CP}$ = 9.7 Hz, C17), 130.1 (s, C4), 130.4 (d, $^1J_{CP}$ = 55.2 Hz, C15), 131.1 (d, $^4J_{CP}$ = 2.0 Hz, C18), 132.2 (d, $^2J_{CP}$ = 8.9 Hz, C16), 154.4 (s, C1). ^{31}P{^{1}H}-NMR (162.0 MHz, $CDCl_3$): δ (ppm) = 11.2 (br m). ESI(+)-MS: *m*/*z* (%) = 479.1 (98.9) $[M + Na]^+$, 456.1 (34.1) $[M]^+$, 422.1 (100) $[M – BH_3]^+$. FT-IR (KBr): $\tilde{\nu}$ (cm^{-1}) = 3925 w, 3422 s, 3082 w, 3056 w, 2956 m, 2929 m, 2868 m, 2377 s, 1886 w, 1611 m, 1591 m, 1527 s, 1483 w, 1457 m, 1437 s, 1383 m, 1362 m, 1263 m, 1216 m, 1172 s, 1106 m, 1065 m, 1030 m, 888 m, 863 w, 831 s, 743 m, 696 m, 629 w, 606 m, 530 m, 494 m. Anal. Calcd. for $C_{26}H_{30}BFeOP$ (456.2): C 68.36, H 6.63; found C 67.88, H 6.79.

Synthesis of Ferrocenyl Phosphines 3a–c

A solution of **2a**–**c** in diethylamine (0.025 mol L^{-1}) was heated at 50 °C for 12 h. Diethylamine was removed by evaporation under reduced pressure and the crude residue was purified by column chromatography on degassed, deactivated silica (pretreated with hexane/triethylamine, 95:5) with degassed hexane/DCM (1:1) grad. DCM. In order to determine the enantiomeric excess, **3a**–**c** was re-protected by BH_3·SMe_2 (2.0 mol L^{-1} in THF) prior analysis by chiral HPLC.

1-[(S_P)-(2-Methoxyphenyl)(phenyl)phosphine]-1′-(4-hydroxyphenyl)ferrocene (3a). Ferrocenyl phosphine **3a** was obtained from ferrocenyl phosphine borane **2a** (0.33 g, 0.66 mmol) as a sticky orange solid (0.31 g, 98 %). Its enantiomeric excess was determined, after reprotection by reaction with BH_3·SMe_2, by analytical chiral HPLC (hexane/2-propanol 85:15, 0.5 mL min^{-1}): *ee* = 92.6 % (t_R:

34.1 min [S_P], 36.8 min [R_P]). R_f: 0.22 (hexane/DCM, 1:2, v/v). mp: 45–47 °C. ^{1}H-NMR (400.2 MHz, $CDCl_3$): δ (ppm) = 3.70–3.71 (m, 1H, H10/H13), 3.71 (s, 3H, H25), 4.07–4.08 (m, 1H, H10/H13), 4.15–4.17 (m, 1H, H11/H12), 4.17–4.18 (m, 1H, H7/8), 4.19–4.20 (m, 1H, H7/8), 4.21–4.22 (m, 1H, H11/H12), 4.42–4.43 (m, 1H, H6/H9), 4.57–4.58 (m, 1H, H6/H9), 4.78 (br s, 1H, OH), 6.71 (d, 2H, $^3J_{HH}$ = 8.6 Hz, H3), 6.81–6.90 (m, 2H, H21, H23), 7.23 (d, 2H, $^3J_{HH}$ = 8.6 Hz, H2), 7.26–7.34 (m, 5H, H16–H18), 7.45–7.49 (m, 2H, H20, H22). ^{13}C{^{1}H}-NMR (100.6 MHz, $CDCl_3$): δ (ppm) = 55.8 (s, C25), 67.1 (s, C6/C9), 67.4 (s, C6/C9), 70.0 (s, C7/C8), 70.1 (s, C7/C8), 72.7 (d, $^3J_{CP}$ = 1.1 Hz, C11/12), 73.4 (d, $^3J_{CP}$ = 5.8 Hz, C11/12), 73.4 (d, $^2J_{CP}$ = 4.6 Hz, C10/C13), 75.9 (d, $^2J_{CP}$ = 24.7 Hz, C10/C13), 76.2 (d, $^1J_{CP}$ = 5.8 Hz, C14), 86.6 (s, C5), 110.4 (d, $^3J_{CP}$ = 1.1 Hz, C23), 115.4 (s, C3), 120.9 (s, C21), 127.6 (s, C2), 128.1 (d, $^2J_{CP}$ = 7.5 Hz, C16), 128.1 (d, $^1J_{CP}$ = 12.7 Hz, C19), 128.6 (s, C18), 130.1 (s, C17), 131.0 (s, C4), 133.8 (s, C20), 134.0 (s, C22), 138.2 (d, $^1J_{CP}$ = 8.1 Hz, C15), 154.1 (s, C1), 160.8 (d, $^2J_{CP}$ = 15.2 Hz, C24). ^{31}P{^{1}H}-NMR (162.0 MHz, $CDCl_3$): δ (ppm) = –29.7 (s). ESI(+)-MS: *m/z* (%) = 531.1 (11.1) $[M + K]^+$, 493.1 (100) $[M + H]^+$. FT-IR (KBr): $\tilde{\nu}$ (cm^{-1}) = 3384 m, 3065 m, 3003 m, 2962 w, 2933 w, 2832 w, 2362 w, 1884 w, 1701 w, 1610 m, 1584 m, 1526 s, 1458 s, 1431 s, 1383 m, 1266 s, 1240 s, 1195 w, 1161 m, 1129 m, 1100 m, 1069 m, 1024 s, 888 m, 829 s, 796 m, 750 s, 698 m, 633 w, 608 w, 575 w, 530 m, 488 m, 434 w. Anal. Calcd. for $C_{29}H_{25}FeO_2P$ (492.1): C 70.75, H 5.12; found C 70.35, H 5.16.

1-[(S_P)-(2-Biphenylyl)(phenyl)phosphine]-1′-(4-hydroxyphenyl)-ferrocene (3b). Ferrocenyl phosphine **3b** was obtained from ferrocenyl phosphine borane **2b** (0.35 g, 0.63 mmol) as a sticky orange solid (0.31 g, 92 %). Its enantiomeric excess was determined, after reprotection by reaction with BH_3 SMe_2, by analytical chiral HPLC (hexane/2-propanol 85:15, 0.5 mL min^{-1}): *ee* = 92.2 % (t_R: 26.7 min [S_P], 41.3 min [R_P]). R_f: 0.25 (hexane/DCM, 1:2, v/v). mp: 52–54 °C. ^{1}H-NMR (400.2 MHz, $CDCl_3$): δ (ppm) = 3.69 (br s, 1H, H11/H12), 3.98 (br s, 1H, H7/H8), 4.08 (br s, 1H, H7/H8), 4.14 (br s, 2H, H10/H13, H11/H12), 4.19 (br s, 2H, H6/H9, H10/H13), 4.48 (br s, 1H, H6/H9), 4.53 (br s, 1H, OH), 6.67 (d, 2H, $^3J_{HH}$ = 8.2 Hz, H3), 7.08–7.12 (m, 3H, H17, H18), 7.11 (d, 2H, $^3J_{HH}$ = 8.0 Hz, H2), 7.18–7.33 (m, 11H, H16, H20–H23, H26–H28). ^{13}C{^{1}H}-NMR (100.6 MHz, $CDCl_3$): δ (ppm) = 67.0 (s, C6/C9), 67.1 (s, C6/C9), 70.0 (s, C7/C8), 70.1 (s, C7/C8), 72.9 (s, C11/C12), 73.3 (s, C11/C12), 73.7 (d, $^2J_{CP}$ = 6.8 Hz, C10/C13), 76.0 (d, $^2J_{CP}$ = 29.9 Hz, C10/C13), 77.1 (d, $^1J_{CP}$ = 8.5 Hz, C14), 86.5 (s, C5), 115.4 (s, C3), 127.0 (s, C2), 127.5 (s, C26), 127.7 (s, C27), 128.0 (s, C23), 128.0 (s, C21), 128.2 (s, C28), 128.6 (s, C22), 129.8 (d, $^3J_{CP}$ = 3.8 Hz, C17), 129.9 (d, $^2J_{CP}$ = 3.8 Hz, C20), 130.9 (s, C4), 132.9 (s, C18), 134.5 (d, $^2J_{CP}$ = 20.5 Hz, C16), 138.4 (d, $^2J_{CP}$ = 8.5 Hz, C24), 139.1 (d, $^1J_{CP}$ = 15.0 Hz, C19), 141.9 (d, $^3J_{CP}$ = 5.0 Hz, C25), 146.9 (d, $^1J_{CP}$ = 24.8 Hz, C15), 154.0 (s, C1). ^{31}P{^{1}H}-NMR (162.0 MHz, $CDCl_3$): δ (ppm) = –23.0 (s). ESI(+)-MS: *m/z* (%) = 538.1 (100) $[M]^+$. FT-IR (KBr): $\tilde{\nu}$ (cm^{-1}) = 3854 w, 3804 w, 3730 w, 3676 w, 3246 m, 3048 m, 2962 m, 2361 m, 2339 m, 1631 w, 1610 w, 1588 w, 1526 s, 1478 w, 1458 m, 1433 s, 1385 w, 1347 w, 1325 w, 1308 w, 1262 s, 1215 m, 1197 m, 1171 m, 1168 m, 1098 s, 1027 s, 916 w, 886 w, 821 s, 803 s, 751 s, 699 s, 672 w, 655 w, 634 w, 611 w, 556 w, 530 w, 488 m, 457 w, 425 w. Anal. Calcd. for $C_{34}H_{27}FeOP$ (538.1): C 75.85, H 5.05; found C 75.18, H 5.16.

1-[(R_P)-(*n*-Butyl)(phenyl)phosphine]-1′-(4-hydroxyphenyl)ferrocene (3c). Ferrocenyl phosphine **3c** was obtained from ferrocenyl phosphine borane **2c** (0.64 g, 1.40 mmol) as a sticky orange solid (0.61 g, 98 %). Its enantiomeric excess was determined, after reprotection by reaction with BH_3•SMe_2, by analytical chiral HPLC (hexane/2-propanol 85:15, 0.5 mL min^{-1}): *ee* = 92.5 % (t_R: 19.9 min [R_P], 22.5 min [S_P]). R_f: 0.23 (hexane/DCM, 1:2, v/v). mp: 41–43 °C. ^{1}H-NMR (400.2 MHz, $CDCl_3$): δ (ppm) = 0.86–0.90 (m, 3H, H22), 1.28–1.51 (m, 4H, H20, H21), 1.81–1.88 (m, 2H, H19), 3.96–3.97 (m, 1H, H10/H13), 4.10–4.11 (m, 1H, H11/H12), 4.14–4.15 (m, 1H, H10/H13), 4.17–4.19 (m, 1H, H11/H12), 4.20–4.23 (m, 2H, H7, H8), 4.48–4.49 (m, 1H, H6/H9), 4.53–4.54 (m, 1H, H6/H9), 4.95 (br s, 1H, OH), 6.76 (d, 2H, $^3J_{HH}$ = 8.6 Hz, H3), 7.28–7.31 (m, 3H, H17, H18), 7.32 (d, 2H, $^3J_{HH}$ = 8.6 Hz, H2), 7.42–7.47 (m, 2H, H16). ^{13}C{^{1}H}-NMR (100.6 MHz, $CDCl_3$): δ (ppm) = 14.0 (s, C22), 24.5 (d, $^2J_{CP}$ = 13.3 Hz, C20), 28.7 (d, $^3J_{CP}$ = 2.9 Hz, C21), 28.7 (d, $^1J_{CP}$ = 21.6 Hz, C19), 67.1 (s, C6/C9), 67.2 (s, C6/C9), 69.9 (s, C7/C8), 69.9 (s, C7/C8), 71.8 (d, $^3J_{CP}$ = 8.0 Hz, C11/12), 72.1 (d, $^3J_{CP}$ = 2.3 Hz, C11/12), 72.7 (d, $^2J_{CP}$ = 4.8 Hz, C10/C13), 74.4 (d, $^2J_{CP}$ = 19.0 Hz, C10/C13), 78.2 (d, $^1J_{CP}$ = 7.7 Hz, C14), 86.6 (s, C5), 115.5 (s, C3), 127.6 (s, C2), 128.3 (d, $^3J_{CP}$ = 7.1 Hz, C17), 128.7 (s, C18), 131.0 (s, C4), 132.9 (d, $^2J_{CP}$ = 19.6 Hz, C16), 140.0 (d, $^1J_{CP}$ = 13.3 Hz, C15), 154.2 (s, C1). ^{31}P{^{1}H}-NMR (162.0 MHz, $CDCl_3$): δ (ppm) = –28.0 (s). ESI(+)-MS: *m/z* (%) = 473.1 (58.9) $[M+CH_3OH]^+$, 443.1 (100) $[M + H]^+$. FT-IR (KBr): $\tilde{\nu}$ (cm^{-1}) = 3418 s, 3443 s, 3023 w, 2955 m, 2926 m, 2854 m, 1876 w, 1610 m, 1596 m, 1525 s, 1448 s, 1377 m, 1241 s, 1175 m, 1159 m, 1101 m, 1068 w, 1028 m, 889 m, 826 s, 741 m, 719 w, 695 m, 634 w, 610 w, 522 m, 491 m. Anal. Calcd. for $C_{26}H_{27}FeOP$ (442.1): C 70.60, H 6.16; found C 70.36, H 6.34.

Synthesis of Dendritic Ferrocenyl Phosphines 3a–c-G_1 and 3a–c-G_2

A solution of **3a–c** (13 equiv. for $\mathbf{G_1}$ or 26 equiv. for $\mathbf{G_2}$) in THF (0.05 mol L^{-1}) was added to dry Cs_2CO_3 (18 equiv. for $\mathbf{G_1}$ or 36 equiv. for $\mathbf{G_2}$) and stirred for 12 h at room temperature. A solution of $\mathbf{G_1}$ or $\mathbf{G_2}$ (1 equiv.) in THF (0.01 mol L^{-1}) was added and stirring resumed until the ^{31}P{^{1}H}-NMR spectrum indicated full conversion (at least 12 h). The suspension was filtered and the filtrate was precipitated with *n*-pentane. After stirring for 15 minutes, the product was isolated and washed twice with *n*-pentane.

Dendritic Ferrocenyl Phosphine 3a-G_1. Dendritic ferrocenyl phosphine **3a-G_1** was obtained from ferrocenyl phosphine **3a** (0.12 g, 0.24 mmol) and $\mathbf{G_1}$ (0.03 g, 0.02 mmol) as an orange solid (0.13 g, 93 %). ^{1}H-NMR (400.2 MHz, $CDCl_3$): δ (ppm) = 3.20 (d, 18H, $^3J_{HP}$ = 10.1 Hz, H34), 3.63 (br s, 48H, H10/H13, H25), 4.01 (br s, 12H, H10/H13), 4.06 (br s, 12H, H11/H12), 4.12 (br s, 12H, H11/H12), 4.14 (br s, 12H, H7/8), 4.16 (br s, 12H, H7/8), 4.34 (br s, 12H, H6/H9), 4.48–4.49 (m, 12H, H6/H9), 6.74–6.84 (m, 36H, H20, H21, H23), 6.98 (d, 12H, $^3J_{HH}$ = 8.7 Hz, H30), 7.01 (d, 24H, $^3J_{HH}$ = 8.2 Hz, H3), 7.17 (d, 24H, $^3J_{HH}$ = 8.5 Hz, H2), 7.18–7.26 (m, 48H, H16, H17), 7.38–7.42 (m, 24H, H18, H22), 7.52 (s, 6H, H33), 7.57 (d, 12H, $^3J_{HH}$ = 8.5 Hz, H31). ^{13}C{^{1}H}-NMR (100.6 MHz, $CDCl_3$): δ (ppm) = 33.2 (d, $^2J_{CP}$ = 11.9 Hz, C34), 55.7 (s, C25), 67.6 (s, C6/C9), 67.8 (s, C6/C9), 70.5 (s, C7/C8), 70.6 (s, C7/C8), 72.8 (s, C11/12), 73.5 (d, $^3J_{CP}$ = 2.8 Hz, C11/12), 73.5 (d, $^2J_{CP}$ = 13.6 Hz, C10/C13), 75.8 (d, $^2J_{CP}$ = 24.6 Hz, C10/C13), 76.5 (d, $^1J_{CP}$ = 6.5 Hz, C14), 85.4 (s, C5), 110.4 (s, C23), 120.9 (s, C21), 121.4 (s, C2), 121.5 (s, C30), 127.3 (s, C3), 128.1 (d, $^1J_{CP}$ = 12.7 Hz, C19), 128.1 (d, $^2J_{CP}$ = 7.7 Hz, C16), 128.4 (s, C31), 128.7 (s, C18), 130.2 (s, C17), 132.4 (s, C32), 133.7 (s, C22), 133.8 (d, $^2J_{CP}$ = 20.3 Hz, C20), 136.1 (s, C4), 138.1 (d, $^1J_{CP}$ = 8.3 Hz, C15), 138.6 (d, $^3J_{CP}$ = 14.3 Hz, C33), 148.9 (d, $^2J_{CP}$ = 7.1 Hz, C1), 151.3 (s, C29), 160.8 (d, $^2J_{CP}$ = 15.2 Hz, C24). ^{31}P{^{1}H}-NMR (162.0 MHz, $CDCl_3$): δ (ppm) = –29.9 (s, (*S*)-P), 8.3 (s, N_3P_3), 62.3 (s, P=S).

Dendritic Ferrocenyl Phosphine 3a-G_2. Dendritic ferrocenyl phosphine **3a-G_2** was obtained from ferrocenyl phosphine **3a** (0.10 g, 0.20 mmol) and $\mathbf{G_2}$ (0.04 g, 0.01 mmol) as an orange solid (0.12 g, 97 %). ^{1}H-NMR (400.2 MHz, $CDCl_3$): δ (ppm) = 3.11 (d, 18H, $^3J_{HP}$ = 9.7 Hz, H34), 3.20 (d, 36H, $^3J_{HP}$ = 9.5 Hz, H40), 3.63 (br s, 96H, H10/H13, H25), 4.01 (br s, 24H, H10/H13), 4.07 (br s, 24H, H11/H12), 4.14 (br s, 72H, H7, H8, H11/H12), 4.36 (br s, 24H, H6/H9), 4.50 (br s, 24H, H6/H9), 6.76–6.89 (m, 84H, H20, H21, H23, H30), 7.02 (d, 48H, $^3J_{HH}$ = 7.05 Hz, H2), 7.15–7.26 (m, 156H, H3, H16, H17, H31), 7.41 (br s, 48H, H18, H22), 7.49 (br s, 18H, H33, H39), 7.56–7.60 (m, 48H, H36, H37).

$^{13}C\{^1H\}$-NMR (100.6 MHz, $CDCl_3$): δ (ppm) = 33.1 (d, $^2J_{CP}$ = 11.3 Hz, C34) = 33.2 (d, $^2J_{CP}$ = 12.8 Hz, C40), 55.7 (s, C25), 67.6 (s, C6/C9), 67.8 (s, C6/C9), 70.5 (s, C7/C8), 70.6 (s, C7/C8), 72.8 (s, C11/12), 73.5 (d, $^3J_{CP}$ = 2.8 Hz, C11/12), 73.5 (d, $^2J_{CP}$ = 12.5 Hz, C10/C13), 75.8 (d, $^2J_{CP}$ = 23.3 Hz, C10/C13), 76.5 (d, $^1J_{CP}$ = 6.4 Hz, C14), 85.4 (s, C5), 110.4 (s, C23), 120.9 (s, C21), 121.5 (s, C2), 121.6 (s, C36), 122.0 (s, C30), 127.3 (s, C3), 128.1 (d, $^1J_{CP}$ = 12.5 Hz, C19), 128.1 (d, $^2J_{CP}$ = 7.4 Hz, C16), 128.5 (s, C31, C37), 128.7 (s, C18), 130.2 (s, C17), 132.6 (s, C32, C38), 133.7 (s, C22), 133.8 (d, $^2J_{CP}$ = 19.8 Hz, C20), 136.1 (s, C4), 138.1 (d, $^1J_{CP}$ = 8.9 Hz, C15), 138.6 (d, $^3J_{CP}$ = 13.5 Hz, C33, C39), 148.9 (d, $^2J_{CP}$ = 6.3 Hz, C1), 151.3 (s, C29), 151.4 (s, C35), 160.8 (d, $^2J_{CP}$ = 15.5 Hz, C24). $^{31}P\{^1H\}$-NMR (162.0 MHz, $CDCl_3$): δ (ppm) = –29.8 (s, (*S*)-P), 8.5 (s, N_3P_3), 62.6 (br s, P=S).

Dendritic Ferrocenyl Phosphine 3b-G$_1$. Dendritic ferrocenyl phosphine **3b-G$_1$** was obtained from ferrocenyl phosphine **3b** (0.12 g, 0.22 mmol) and **G$_1$** (0.03 g, 0.02 mmol) as an orange solid (0.12 g, 89 %). ^{1}H-NMR (400.2 MHz, [D$_8$]THF): δ (ppm) = 3.23 (d, 18H, $^3J_{HP}$ = 10.3 Hz, H34), 3.58 (br s, 12H, H11/H12), 3.96 (br s, 12H, H7/H8), 4.00 (br s, 12H, H10/H13), 4.05 (br s, 24H, H7/H8, H11/H12), 4.09 (br s, 12H, H10/H13), 4.24 (br s, 12H, H6/H9), 4.49–4.51 (m, 12H, H6/H9), 7.01–7.28 (m, 228H, H2, H3, H16–H18, H20–H23, H26–H28, H30), 7.64 (s, 6H, H33), 7.66 (br s, 12H, H31). $^{13}C\{^1H\}$-NMR (100.6 MHz, [D$_8$]THF): δ (ppm) = 33.7 (d, $^2J_{CP}$ = 11.3 Hz, C34), 68.3 (s, C6/C9), 68.4 (s, C6/C9), 71.3 (s, C7/C8), 71.5 (s, C7/C8), 73.6 (s, C11/C12), 74.2 (s, C11/C12), 74.6 (d, $^2J_{CP}$ = 5.2 Hz, C10/C13), 76.7 (d, $^2J_{CP}$ = 28.1 Hz, C10/C13), 78.7 (d, $^1J_{CP}$ = 10.5 Hz, C14), 86.3 (s, C5), 122.2 (s, C2), 122.4 (s, C30), 127.8 (s, C3), 128.0 (s, C26), 128.4 (s, C27), 128.9 (s, C23), 128.9 (s, C21), 129.1 (s, C28), 129.3 (s, C31), 129.4 (s, C22), 130.8 (d, $^2J_{CP}$ = 3.7 Hz, C20), 130.8 (d, $^3J_{CP}$ = 3.9 Hz, C17), 133.7 (s, C32), 134.0 (s, C18), 135.4 (d, $^2J_{CP}$ = 20.6 Hz, C16), 137.0 (s, C4), 139.6 (d, $^3J_{CP}$ = 11.6 Hz, C33), 139.9 (d, $^2J_{CP}$ = 7.3 Hz, C24), 139.9 (d, $^1J_{CP}$ = 35.1 Hz, C19), 143.1 (d, $^3J_{CP}$ = 4.9 Hz, C25), 148.2 (d, $^1J_{CP}$ = 25.8 Hz, C15), 150.2 (d, $^2J_{CP}$ = 7.0 Hz, C1), 152.5 (d, $^2J_{CP}$ = 4.9 Hz, C29). $^{31}P\{^1H\}$-NMR (162.0 MHz, [D$_8$]THF): δ (ppm) = –24.0 (s, (*S*)-P), 8.4 (s, N_3P_3), 62.2 (s, P=S).

Dendritic Ferrocenyl Phosphine 3b-G$_2$. Dendritic ferrocenyl phosphine **3b-G$_2$** was obtained from ferrocenyl phosphine **3b** (0.10 g, 0.19 mmol) and **G$_2$** (0.03 g, 0.01 mmol) as an orange solid (0.11 g, 91 %). ^{1}H-NMR (400.2 MHz, [D$_8$]THF): δ (ppm) = 3.20 (d, 18H, $^3J_{HP}$ = 9.8 Hz, H34), 3.22 (d, 36H, $^3J_{HP}$ = 10.2 Hz, H40), 3.59 (br s, 24H, H11/H12), 3.95 (br s, 24H, H7/H8), 4.00 (br s, 24H, H10/H13), 4.04 (br s, 24H, H7/H8), 4.05 (br s, 24H, H11/H12), 4.10 (br s, 24H, H10/H13), 4.24 (br s, 24H, H6/H9), 4.50 (m, 24H, H6/H9), 6.97–7.28 (m, 468H, H2, H3, H16–H18, H20–H23, H26–H28, H30, H36), 7.63–7.68 (m, 54H, H31, H33, H37, H39). $^{13}C\{^1H\}$-NMR (100.6 MHz, [D$_8$]THF): δ (ppm) = 33.7 (d, $^2J_{CP}$ = 12.0 Hz, C34, C40), 68.3 (s, C6/C9), 68.5 (s, C6/C9), 71.3 (s, C7/C8), 71.5 (s, C7/C8), 73.6 (s, C11/C12), 74.3 (s, C11/C12), 74.6 (d, $^2J_{CP}$ = 6.3 Hz, C10/C13), 76.7 (d, $^2J_{CP}$ = 27.3 Hz, C10/C13), 78.7 (d, $^1J_{CP}$ = 10.4 Hz, C14), 86.3 (s, C5), 122.3 (s, C2, C36), 122.9 (s, C30), 127.8 (s, C37), 127.9 (s, C3), 128.0 (s, C26), 128.4 (s, C27), 128.9 (s, C23), 129.0 (s, C21), 129.1 (s, C28), 129.3 (s, C31), 129.5 (s, C22), 130.8 (d, $^3J_{CP}$ = 3.8 Hz, C17, C20), 133.9 (s, C38), 134.0 (s, C32), 134.0 (s, C18), 135.3 (d, $^2J_{CP}$ = 20.5 Hz, C16), 136.9 (s, C4), 139.8 (d, $^3J_{CP}$ = 12.4 Hz, C33, C39), 139.9 (d, $^2J_{CP}$ = 7.2 Hz, C24), 139.9 (d, $^1J_{CP}$ = 35.4 Hz, C19), 143.0 (d, $^3J_{CP}$ = 4.8 Hz, C25), 148.1 (d, $^1J_{CP}$ = 25.9 Hz, C15), 150.1 (d, $^2J_{CP}$ = 6.9 Hz, C1, C35), 152.5 (d, $^2J_{CP}$ = 6.7 Hz, C29). $^{31}P\{^1H\}$-NMR (162.0 MHz, [D$_8$]THF): δ (ppm) = –24.2 (s, (*S*)-P), 8.2 (s, N_3P_3), 62.2 (br s, P=S).

Dendritic Ferrocenyl Phosphine 3c-G$_1$. Dendritic ferrocenyl phosphine **3c-G$_1$** was obtained from ferrocenyl phosphine **3c** (0.20 g, 0.45 mmol) and **G$_1$** (0.06 g, 0.04 mmol) as an orange solid (0.22 g, 96 %). ^{1}H-NMR (400.2 MHz, [D$_8$]THF): δ (ppm) = 0.84–0.88 (m, 36H, H22), 1.28–1.47 (m, 48H, H20, H21), 1.83–1.86 (m, 24H, H19), 3.28 (d, 18H, $^3J_{HP}$ = 10.2 Hz, H34), 3.88 (br s, 12H, H10/H13), 4.03 (br s, 12H, H10/H13), 4.09 (br s, 12H, H11/H12), 4.13 (br s, 12H, H11/H12), 4.20 (br s, 24H, H7, H8), 4.50–4.51 (m, 12H, H6/H9), 4.56–4.57 (m, 12H, H6/H9), 7.08 (d, 12H, $^3J_{HH}$ = 8.5 Hz, H30), 7.12 (d, 24H, $^3J_{HH}$ = 8.1 Hz, H2), 7.22–7.23 (m, 36H, H17, H18), 7.38–7.43 (m, 48H, H3, H16), 7.68 (d, 12H, $^3J_{HH}$ = 8.7 Hz, H31), 7.70 (s, 6H, H33). $^{13}C\{^1H\}$-NMR (100.6 MHz, [D$_8$]THF): δ (ppm) = 14.5 (s, C22), 25.3 (d, $^2J_{CP}$ = 13.0 Hz, C20), 29.7 (d, $^3J_{CP}$ = 3.2 Hz, C21), 29.7 (d, $^1J_{CP}$ = 30.6 Hz, C19), 33.7 (d, $^2J_{CP}$ = 12.1 Hz, C34), 68.2 (s, C6/C9), 68.6 (s, C6/C9), 71.1 (s, C7/C8), 71.2 (s, C7/C8), 72.6 (d, $^3J_{CP}$ = 8.2 Hz, C11/12), 73.0 (s, C11/12), 73.6 (d, $^2J_{CP}$ = 4.0 Hz, C10/C13), 75.5 (d, $^2J_{CP}$ = 19.3 Hz, C10/C13), 78.0 (d, $^1J_{CP}$ = 10.9 Hz, C14), 86.3 (s, C5), 122.3 (s, C30), 122.3 (s, C2), 128.1 (s, C3), 129.0 (d, $^3J_{CP}$ = 7.0 Hz, C17), 129.3 (s, C31), 129.5 (s, C18), 133.8 (s, C32), 133.9 (d, $^2J_{CP}$ = 20.2 Hz, C16), 137.2 (s, C4), 139.9 (d, $^3J_{CP}$ = 12.1 Hz, C33), 141.5 (d, $^1J_{CP}$ = 15.8 Hz, C15), 150.3 (d, $^2J_{CP}$ = 7.2 Hz, C1), 152.5 (d, $^2J_{CP}$ = 2.6 Hz, C29). $^{31}P\{^1H\}$-NMR (162.0 MHz, [D$_8$]THF): δ (ppm) = –29.1 (s, (*S*)-P), 8.4 (s, N_3P_3), 62.2 (s, P=S).

Dendritic Ferrocenyl Phosphine 3c-G$_2$. Dendritic ferrocenyl phosphine **3c-G$_2$** was obtained from ferrocenyl phosphine **3c** (0.20 g, 0.45 mmol) and **G$_2$** (0.08 g, 0.02 mmol) as an orange solid (0.23 g, 92 %). ^{1}H-NMR (400.2 MHz, [D$_8$]THF): δ (ppm) = 0.83–0.87 (m, 72H, H22), 1.27–1.45 (m, 96H, H20, H21), 1.82–1.84 (m, 48H, H19), 3.24 (d, 18H, $^3J_{HP}$ = 10.4 Hz, H34), 3.28 (d, 36H, $^3J_{HP}$ = 10.4 Hz, H40), 3.87 (br s, 24H, H10/H13), 4.03 (br s, 24H, H10/H13), 4.09 (br s, 24H, H11/H12), 4.12 (br s, 24H, H11/H12), 4.19 (br s, 48H, H7, H8), 4.50 (br s, 24H, H6/H9), 4.56 (br s, 24H, H6/H9), 7.00 (d, 12H, $^3J_{HH}$ = 7.9 Hz, H30), 7.12 (d, 48H, $^3J_{HH}$ = 7.9 Hz, H2), 7.21–7.25 (m, 96H, H17, H18, H36), 7.39–7.40 (m, 96H, H3, H16), 7.64–7.71 (m, 54H, H31, H33, H37, H39). $^{13}C\{^1H\}$-NMR (100.6 MHz, [D$_8$]THF): δ (ppm) = 14.5 (s, C22), 25.3 (d, $^2J_{CP}$ = 13.1 Hz, C20), 29.7 (d, $^3J_{CP}$ = 3.7 Hz, C21), 29.7 (d, $^1J_{CP}$ = 31.2 Hz, C19), 33.7 (d, $^2J_{CP}$ = 12.4 Hz, C34, C40), 68.2 (s, C6/C9), 68.6 (s, C6/C9), 71.1 (s, C7, C8), 72.6 (br s, C11/12), 73.0 (s, C11/12), 73.6 (br s, C10/C13), 75.5 (d, $^2J_{CP}$ = 19.3 Hz, C10/C13), 80.0 (d, $^1J_{CP}$ = 10.9 Hz, C14), 86.3 (s, C5), 122.4 (s, C36), 122.4 (s, C2), 122.8 (s, C30), 128.1 (s, C3), 129.0 (d, $^3J_{CP}$ = 7.0 Hz, C17), 129.3 (s, C37), 129.4 (s, C31), 129.5 (s, C18), 133.6 (s, C38), 133.9 (s, C32), 133.8 (d, $^2J_{CP}$ = 20.1 Hz, C16), 137.1 (s, C4), 139.9 (d, $^3J_{CP}$ = 13.3 Hz, C33, C39), 141.5 (d, $^1J_{CP}$ = 15.7 Hz, C15), 150.3 (d, $^2J_{CP}$ = 7.1 Hz, C1), 152.6 (d, $^2J_{CP}$ = 6.4 Hz, C29, C35). $^{31}P\{^1H\}$-NMR (162.0 MHz, [D$_8$]THF): δ (ppm) = –29.1 (s, (*S*)-P), 8.4 (s, N_3P_3), 62.4 (br s, P=S).

Synthesis of Dendritic Ruthenium(II) Complexes 3a–c-G$_1$-Ru and 3a–c-G$_2$-Ru

A solution of di-μ-chlorobis[(η^6-*p*-cymene)chlororuthenium(II)] (6 equiv. for **3a–c-G$_1$** or 12 equiv. for **3a–c-G$_2$**) in DCM (0.05 mol L^{-1}) was added to a solution of **3a–c-G$_1$** and **3a–c-G$_2$** (1.00 equiv.) in DCM (0.01 mol L^{-1}) and stirred at room temperature until the $^{31}P\{^1H\}$-NMR spectrum indicated full conversion (**3b-G$_1$-Ru** and **3b-G$_2$-Ru** were exposed to the light of a conventional desk lamp while stirring to support *p*-cymene substitution). The solution was concentrated and precipitated with a mixture of hexane/DCM (3:1). After stirring for 15 minutes, the product was isolated and washed twice with hexane.

Dendritic Ruthenium Complex 3a-G$_1$-Ru. Dendritic ruthenium complex **3a-G$_1$-Ru** was obtained from dendritic ferrocenyl phosphine **3a-G$_1$** (0.11 g, 0.02 mmol) as an orange solid (0.16 g, 94 %). ^{1}H-NMR (400.2 MHz, CD_2Cl_2): δ (ppm) = 0.36 (d, 36H, $^3J_{HH}$ = 6.5 Hz, H49/H50), 0.95 (d, 36H, $^3J_{HH}$ = 7.0 Hz, H49/H50), 2.06 (s, 36H, H41), 2.50 (sept, 12H, $^3J_{HH}$ = 6.8 Hz, H48), 3.23 (d, 18H, $^3J_{HP}$ = 10.0 Hz, H34), 3.49 (s, 36H, H25), 3.62 (br s, 12H, H7/H8), 3.73 (br s, 12H, H6/H9), 3.80 (br s, 12H, H10/H13), 3.83 (br s, 12H, H7/H8), 3.95 (br s,

12H, H11/12), 4.09 (br s, 12H, H11/12), 4.20 (br s, 12H, H6/H9), 4.76 (m, 12H, H10/H13), 4.83 (d, 12H, $^3J_{HH}$ = 5.2 Hz, H45/46), 5.13 (br s, 12H, H43/H44), 5.38 (d, 12H, $^3J_{HH}$ = 6.4 Hz, H45/H46), 5.52 (d, 12H, $^3J_{HH}$ = 6.4 Hz, H43/H44), 6.85 (t, 12H, $^3J_{HH}$ = 7.5 Hz, H21), 6.89–6.92 (m, 12H, H23), 6.97 (d, 36H, $^3J_{HH}$ = 8.0 Hz, H2, H30), 7.10 (d, 24H, $^3J_{HH}$ = 7.7 Hz, H3), 7.18–7.22 (m, 12H, H20), 7.34 (t, 12H, $^3J_{HH}$ = 7.7 Hz, H22), 7.41–7.47 (m, 36H, H17, H18), 7.61–7.63 (m, 18H, H31, H33), 7.81–7.85 (m, 24H, H16). $^{13}C\{^1H\}$-NMR (100.6 MHz, CD_2Cl_2): δ (ppm) = 17.7 (s, C41), 18.8 (s, C49/C50), 23.6 (s, C49/C50), 30.3 (s, C48), 33.7 (d, $^2J_{CP}$ = 11.7 Hz, C34), 55.2 (s, C25), 67.7 (s, C6/C9), 68.2 (s, C6/C9), 72.6 (d, $^3J_{CP}$ = 7.6 Hz, C11/C12), 73.5 (s, C7, C8), 73.7 (d, $^2J_{CP}$ = 6.4 Hz, C10/C13), 75.0 (s, C11/12), 77.7 (d, $^1J_{CP}$ = 52.0 Hz, C14), 80.2 (d, $^2J_{CP}$ = 12.7 Hz, C10/C13), 81.3 (s, C45/C46), 85.3 (s, C5), 87.3 (s, C43/C44), 90.7 (d, $^2J_{CP}$ = 10.4 Hz, C45/C46), 94.0 (s, C42), 96.5 (d, $^2J_{CP}$ = 4.8 Hz, C43/C44), 108.3 (s, C47), 111.7 (d, $^3J_{CP}$ = 3.6 Hz, C23), 120.9 (d, $^3J_{CP}$ = 9.4 Hz, C21), 121.6 (s, C2), 121.8 (s, C30), 126.5 (d, $^1J_{CP}$ = 44.3 Hz, C19), 127.6 (s, C3), 127.6 (d, $^3J_{CP}$ = 9.7 Hz, C17), 128.9 (s, C31), 130.2 (s, C18), 132.2 (s, C22), 132.9 (s, C32), 133.3 (d, $^2J_{CP}$ = 9.4 Hz, C16), 136.5 (s, C4), 137.6 (d, $^1J_{CP}$ = 49.2 Hz, C15), 137.7 (d, $^2J_{CP}$ = 7.9 Hz, C20), 139.5 (d, $^3J_{CP}$ = 12.3 Hz, C33), 149.2 (d, $^2J_{CP}$ = 5.3 Hz, C1), 151.7 (s, C29), 158.9 (s, C24). $^{31}P\{^1H\}$-NMR (162.0 MHz, CD_2Cl_2): δ (ppm) = 8.6 (s, N_3P_3), 17.1 (br s, (*S*)-P-Ru), 62.6 (s, P=S).

Dendritic Ruthenium Complex 3a-G$_2$-Ru. Dendritic ruthenium complex **3a-G$_2$-Ru** was obtained from dendritic ferrocenyl phosphine **3a-G$_2$** (0.11 g, 0.01 mmol) as an orange solid (0.15 g, 95 %). ^{1}H-NMR (400.2 MHz, CD_2Cl_2): δ (ppm) = 0.34 (d, 72H, $^3J_{HH}$ = 5.3 Hz, H49/H50), 0.93 (d, 72H, $^3J_{HH}$ = 6.3 Hz, H49/H50), 2.03 (s, 72H, H41), 2.49 (sept, 24H, $^3J_{HH}$ = 6.8 Hz, H48), 3.19–3.24 (m, 54H, H34, H40), 3.47 (s, 72H, H25), 3.59 (br s, 24H, H7/H8), 3.76 (br s, 24H, H6/H9), 3.82 (br s, 48H, H7/H8, H10/H13), 3.93 (br s, 24H, H11/12), 4.09 (br s, 24H, H11/12), 4.20 (br s, 24H, H6/H9), 4.75 (m, 24H, H10/H13), 4.82 (br s, 24H, H45/46), 5.11 (br s, 24H, H43/H44), 5.36 (br s, 24H, H45/H46), 5.50 (br s, 24H, H43/H44), 6.81–6.90 (m, 48H, H21, H23), 6.98 (d, 48H, $^3J_{HH}$ = 7.7 Hz, H2), 7.10–7.20 (m, 108H, H3, H20, H30, H36), 7.32 (t, 24H, $^3J_{HH}$ = 6.9 Hz, H22), 7.42 (br s, 72H, H17, H18), 7.62–7.67 (m, 54H, H31, H33, H37, H39), 7.82 (br s, 48H, H16). $^{13}C\{^1H\}$-NMR (100.6 MHz, CD_2Cl_2): δ (ppm) = 17.7 (s, C41), 18.9 (s, C49/C50), 23.6 (s, C49/C50), 30.3 (s, C48), 33.7 (d, $^2J_{CP}$ = 12.2 Hz, C34, C40), 55.3 (s, C25), 67.7 (s, C6/C9), 68.3 (s, C6/C9), 72.7 (s, C11/C12), 73.3 (s, C7/C8), 73.4 (s, C7/C8), 73.6 (d, $^2J_{CP}$ = 8.5 Hz, C10/C13), 75.1 (s, C11/12), 77.7 (d, $^1J_{CP}$ = 51.6 Hz, C14), 80.3 (d, $^2J_{CP}$ = 13.6 Hz, C10/C13), 81.3 (s, C45/C46), 85.4 (s, C5), 87.3 (s, C43/C44), 90.8 (s, C45/C46), 94.0 (s, C42), 96.6 (s, C43/C44), 108.3 (s, C47), 111.8 (s, C23), 121.0 (d, $^3J_{CP}$ = 8.5 Hz, C21), 121.7 (s, C2), 121.9 (s, C36), 122.4 (s, C30), 126.5 (d, $^1J_{CP}$ = 45.5 Hz, C19), 127.6 (s, C3), 127.7 (d, $^3J_{CP}$ = 9.5 Hz, C17), 129.0 (s, C31, C37), 130.3 (s, C18), 132.3 (s, C22), 133.1 (s, C32, C38), 133.3 (d, $^2J_{CP}$ = 10.4 Hz, C16), 136.5 (s, C4), 137.7 (d, $^1J_{CP}$ = 50.5 Hz, C15), 137.8 (d, $^2J_{CP}$ = 5.5 Hz, C20), 139.7 (d, $^3J_{CP}$ = 13.3 Hz, C33, C39), 149.3 (d, $^2J_{CP}$ = 5.5 Hz, C1), 151.8 (s, C29), 151.8 (s, C35), 159.0 (s, C24). $^{31}P\{^1H\}$-NMR (162.0 MHz, CD_2Cl_2): δ (ppm) = 8.3 (s, N_3P_3), 17.1 (br s, (*S*)-P-Ru), 62.7 (br s, P=S).

Dendritic Ruthenium Complex 3b-G$_1$-Ru. Dendritic ruthenium complex **3b-G$_1$-Ru** was obtained from dendritic ferrocenyl phosphine **3b-G$_1$** (0.10 g, 0.01 mmol) as an orange solid (0.12 g, 95 %). Light activation by a conventional desk lamp enabled the tethering process while stirring. ^{1}H-NMR (400.2 MHz, CD_2Cl_2): δ (ppm) = 3.28 (d, 18H, $^3J_{HP}$ = 9.0 Hz, H34), 3.96 (br s, 12H, H11/H12), 4.10 (br s, 12H, H10/H13), 4.14 (br s, 24H, H7/H8, H10/H13), 4.21 (br s, 12H, H7/H8), 4.31 (br s, 12H, H6/H9), 4.48 (br s, 12H, H6/H9), 4.55 (br s, 12H, H11/H12), 4.90 (d, 12H, $^3J_{HH}$ = 4.4 Hz, H26/H42), 5.17 (d, 12H, $^3J_{HH}$ = 4.5 Hz, H26/H42), 5.86 (br s, 24H, H27, H41), 6.22 (br s, 12H, H28), 7.01 (d, 12H, $^3J_{HH}$ = 7.7 Hz, H30), 7.09 (d, 24H, $^3J_{HH}$ = 7.6 Hz, H2), 7.24–7.29 (m, 48H, H3, H21, H31), 7.35–7.43 (m, 36H, H16, H23), 7.52 (br s, 24H, H18, H20), 7.58–7.69 (m, 42H, H17, H22, H33). $^{13}C\{^1H\}$-NMR (100.6 MHz, CD_2Cl_2): δ (ppm) = 33.9 (d, $^2J_{CP}$ = 9.8 Hz, C34), 68.7 (s, C6/C9), 69.2 (s, C6/C9), 72.2 (s, C7/C8), 72.5 (s, C7/C8), 72.6 (d, $^2J_{CP}$ = 8.3 Hz, C10/C13), 75.5 (s, C10/C13, C11/C12), 76.7 (s, C11/C12), 76.9 (d, $^1J_{CP}$ = 45.9 Hz, C14), 81.4 (s, C26/C42), 82.0 (s, C26/C42), 86.7 (s, C5), 91.4 (d, $^2J_{CP}$ = 12.7 Hz, C28), 97.8 (s, C27/C41), 98.4 (s, C27/C41), 109.7 (s, C25), 122.0 (s, C2, C30), 127.8 (s, C21), 128.0 (d, $^3J_{CP}$ = 10.9 Hz, C17), 128.2 (s, C3), 129.0 (s, C31), 130.3 (s, C20), 130.7 (s, C23), 132.1 (s, C22), 132.7 (d, $^2J_{CP}$ = 8.7 Hz, C16), 133.0 (s, C32), 133.4 (d, $^1J_{CP}$ = 50.4 Hz, C15), 133.5 (s, C18), 136.0 (s, C4), 139.9 (d, $^3J_{CP}$ = 13.8 Hz, C33), 144.5 (d, $^2J_{CP}$ = 23.7 Hz, C24), 145.6 (d, $^1J_{CP}$ = 52.4 Hz, C19), 149.7 (d, $^2J_{CP}$ = 7.0 Hz, C1), 151.8 (d, $^2J_{CP}$ = 6.7 Hz, C29). $^{31}P\{^1H\}$-NMR (162.0 MHz, CD_2Cl_2): δ (ppm) = 8.4 (s, N_3P_3), 43.2 (br s, (*S*)-P-Ru), 62.5 (s, P=S).

Dendritic Ruthenium Complex 3b-G$_2$-Ru. Dendritic ruthenium complex **3b-G$_2$-Ru** was obtained from dendritic ferrocenyl phosphine **3b-G$_2$** (0.10 g, 0.01 mmol) as an orange solid (0.12 g, 92 %). Light activation by a conventional desk lamp enabled the tethering process while stirring. ^{1}H-NMR (400.2 MHz, CD_2Cl_2): δ (ppm) = 3.20 (br s, 18H, H34), 3.27 (br s, 36H, H40), 3.95 (br s, 24H, H11/H12), 4.10 (br s, 24H, H10/H13), 4.12 (br s, 48H, H7/H8, H10/H13), 4.17 (br s, 24H, H7/H8), 4.28 (br s, 24H, H6/H9), 4.46 (br s, 24H, H6/H9), 4.52 (br s, 24H, H11/H12), 4.88 (br s, 24H, H26/H42), 5.14 (br s, 24H, H26/H42), 5.80–5.83 (m, 48H, H27, H41), 6.18 (br s, 24H, H28), 6.90–7.01 (m, 36H, H30, H36), 7.08 (d, 48H, $^3J_{HH}$ = 6.6 Hz, H2), 7.15–7.38 (m, 180H, H3, H16, H21, H23, H31, H37), 7.50–7.65 (m, 138H, H17, H18, H20, H22, H33, H39). $^{13}C\{^1H\}$-NMR (100.6 MHz, CD_2Cl_2): δ (ppm) = 33.9 (d, $^2J_{CP}$ = 8.6 Hz, C34, C40), 68.8 (s, C6/C9), 69.2 (s, C6/C9), 72.2 (s, C7/C8), 72.4 (s, C7/C8), 72.6 (d, $^2J_{CP}$ = 5.6 Hz, C10/C13), 75.4 (s, C10/C13, C11/C12), 76.6 (s, C11/C12), 77.0 (d, $^1J_{CP}$ = 49.0 Hz, C14), 81.4 (s, C26/C42), 82.0 (s, C26/C42), 86.7 (s, C5), 91.5 (d, $^2J_{CP}$ = 17.7 Hz, C28), 97.6 (s, C27/C41), 98.4 (s, C27/C41), 109.8 (s, C25), 121.8 (s, C30), 122.1 (s, C2), 122.4 (s, C36), 128.0 (s, C21), 128.1 (d, $^3J_{CP}$ = 10.8 Hz, C17), 128.2 (s, C3), 129.0 (s, C37), 129.1 (s, C31), 130.3 (s, C20), 130.7 (s, C23), 132.1 (s, C22), 132.7 (d, $^2J_{CP}$ = 8.4 Hz, C16), 134.2 (s, C32), 134.3 (s, C38), 133.3 (d, $^1J_{CP}$ = 53.5 Hz, C15), 133.5 (s, C18), 136.0 (s, C4), 140.0 (br s, C33, C39), 144.5 (d, $^2J_{CP}$ = 22.4 Hz, C24), 145.6 (d, $^1J_{CP}$ = 48.2 Hz, C19), 149.7 (d, $^2J_{CP}$ = 6.2 Hz, C1), 151.8 (d, $^2J_{CP}$ = 10.7 Hz, C29, C35). $^{31}P\{^1H\}$-NMR (162.0 MHz, CD_2Cl_2): δ (ppm) = 8.4 (s, N_3P_3), 43.4 (br s, (*S*)-P-Ru), 62.6 (s, P=S).

Dendritic Ruthenium Complex 3c-G$_1$-Ru. Dendritic ruthenium complex **3c-G$_1$-Ru** was obtained from dendritic ferrocenyl phosphine **3c-G$_1$** (0.20 g, 0.03 mmol) as an orange solid (0.23 g, 74 %). The solution was precipitated with a mixture of hexane/DCM (4:1). ^{1}H-NMR (400.2 MHz, CD_2Cl_2): δ (ppm) = 0.80 (t, 36H, $^3J_{HH}$ = 7.0 Hz, H22), 0.92 (d, 36H, $^3J_{HH}$ = 6.7 Hz, H49/H50), 0.96 (d, 36H, $^3J_{HH}$ = 6.9 Hz, H49/H50), 1.22–1.32 (m, 48H, H20, H21), 1.55 (s, 36H, H41), 2.18–2.32 (m, 24H, H19), 2.74–2.83 (m, 12H, H48), 3.37 (d, 18H, $^3J_{HP}$ = 10.1 Hz, H34), 4.21 (br s, 12H, H11/H12), 4.30 (br s, 24H, H10/H13, H11/H12), 4.34 (br s, 24H, H7, H8), 4.45 (br s, 12H, H10/H13), 4.64 (br s, 12H, H6/H9), 4.67 (br s, 12H, H6/H9), 4.92 (d, 12H, $^3J_{HH}$ = 5.2 Hz, H45/H46), 4.95 (d, 12H, $^3J_{HH}$ = 4.8 Hz, H43/H44), 5.05 (d, 12H, $^3J_{HH}$ = 5.8 Hz, H43/H44), 5.12 (d, 12H, $^3J_{HH}$ = 5.9 Hz, H45/H46), 7.04 (d, 12H, $^3J_{HH}$ = 8.4 Hz, H30), 7.18 (d, 24H, $^3J_{HH}$ = 8.2 Hz, H2), 7.42–7.44 (m, 60H, H3, H17, H18), 7.71 (d, 12H, $^3J_{HH}$ = 8.5 Hz, H31), 7.77 (br s, 6H, H33), 8.05–8.09 (m, 24H, H16). $^{13}C\{^1H\}$-NMR (100.6 MHz, CD_2Cl_2): δ (ppm) = 14.3 (s, C22), 17.7 (s, C41), 21.9 (s, C49/C50), 22.8 (s, C49/C50), 24.9 (d, $^2J_{CP}$ = 13.1 Hz, C20), 26.0 (d, $^1J_{CP}$ = 30.0 Hz, C19), 27.2 (d, $^3J_{CP}$ = 7.6 Hz, C21), 30.7 (s, C48), 33.8 (d, $^2J_{CP}$ = 11.4 Hz, C34), 68.5 (s, C6/C9), 69.1 (s, C6/C9), 72.3 (s, C7/C8), 72.6 (s, C7/C8), 73.9 (d, $^3J_{CP}$ = 7.9 Hz, C11/12), 74.1 (d, $^2J_{CP}$ = 6.9 Hz, C10/13), 74.4 (d, $^3J_{CP}$ = 6.2 Hz, C11/12), 75.0 (d, $^2J_{CP}$ = 12.7 Hz, C10/13), 78.8 (d, $^1J_{CP}$ = 44.1 Hz, C14), 84.6 (d, $^2J_{CP}$ = 2.2 Hz, C45/C46), 86.3 (d, $^2J_{CP}$ =

6.5 Hz, C45/C46), 86.5 (s, C5), 89.1 (d, $^2J_{CP}$ = 4.5 Hz, C43/C44), 90.7 (d, $^2J_{CP}$ = 2.9 Hz, C43/C44), 95.0 (s, C42), 108.3 (s, C47), 121.9 (d, $^3J_{CP}$ = 4.1 Hz, C30), 122.1 (d, $^3J_{CP}$ = 3.9 Hz, C2), 128.1 (s, C3), 128.5 (d, $^3J_{CP}$ = 9.5 Hz, C17), 129.0 (s, C31), 130.6 (d, $^4J_{CP}$ = 2.0 Hz, C18), 132.9 (d, $^2J_{CP}$ = 8.4 Hz, C16), 133.0 (s, C32), 135.0 (d, $^1J_{CP}$ = 43.2 Hz, C15), 135.9 (s, C4), 139.7 (d, $^3J_{CP}$ = 12.2 Hz, C33), 149.9 (d, $^2J_{CP}$ = 7.0 Hz, C1), 151.8 (s, C29). $^{31}P\{^1H\}$-NMR (162.0 MHz, CD_2Cl_2): δ (ppm) = 8.4 (s, N_3P_3), 15.0 (br s, (*R*)-P-Ru), 62.6 (s, P=S).

Dendritic Ruthenium Complex 3c-G_2-Ru. Dendritic ruthenium complex **3c-G_2-Ru** was obtained from dendritic ferrocenyl phosphine **3c-G_2** (0.20 g, 0.01 mmol) as an orange solid (0.29 g, 95 %). The solution was precipitated with a mixture of hexane/DCM (6:1). ^{1}H-NMR (400.2 MHz, CD_2Cl_2): δ (ppm) = 0.78 (t, 72H, $^3J_{HH}$ = 6.7 Hz, H22), 0.91 (d, 72H, $^3J_{HH}$ = 6.8 Hz, H49/H50), 0.95 (d, 72H, $^3J_{HH}$ = 6.9 Hz, H49/H50), 1.20–1.29 (m, 96H, H20, H21), 1.53 (s, 72H, H41), 2.17–2.30 (m, 48H, H19), 2.73–2.82 (m, 24H, H48), 3.28 (d, 18H, $^3J_{HP}$ = 9.9 Hz, H34), 3.37 (d, 36H, $^3J_{HP}$ = 10.1 Hz, H40), 4.22 (br s, 24H, H11/H12), 4.29 (br s, 48H, H10/H13, H11/H12), 4.33 (br s, 48H, H7, H8), 4.44 (br s, 24H, H10/H13), 4.65 (br s, 24H, H6/H9), 4.68 (br s, 24H, H6/H9), 4.90 (d, 24H, $^3J_{HH}$ = 5.3 Hz, H45/H46), 4.94 (d, 24H, $^3J_{HH}$ = 4.6 Hz, H43/H44), 5.04 (d, 24H, $^3J_{HH}$ = 5.8 Hz, H43/H44), 5.11 (d, 24H, $^3J_{HH}$ = 5.6 Hz, H45/H46), 7.00 (d, 12H, $^3J_{HH}$ = 8.1 Hz, H30), 7.18 (d, 48H, $^3J_{HH}$ = 8.2 Hz, H2), 7.21 (d, 24H, $^3J_{HH}$ = 9.6 Hz, H36), 7.41–7.46 (m, 120H, H3, H17, H18), 7.66 (d, 12H, $^3J_{HH}$ = 8.2 Hz, H31), 7.72–7.74 (m, 42H, H33, H37, H39), 8.05–8.09 (m, 48H, H16). $^{13}C\{^1H\}$-NMR (100.6 MHz, CD_2Cl_2): δ (ppm) = 14.3 (s, C22), 17.7 (s, C41), 21.9 (s, C49/C50), 22.8 (s, C49/C50), 24.9 (d, $^2J_{CP}$ = 13.1 Hz, C20), 25.9 (d, $^1J_{CP}$ = 30.3 Hz, C19), 27.2 (d, $^3J_{CP}$ = 7.4 Hz, C21), 30.7 (s, C48), 33.8 (d, $^2J_{CP}$ = 11.8 Hz, C34, C40), 68.5 (s, C6/C9), 69.1 (s, C6/C9), 72.3 (s, C7/C8), 72.6 (s, C7/C8), 73.8 (d, $^3J_{CP}$ = 7.1 Hz, C11/12), 74.1 (d, $^2J_{CP}$ = 6.0 Hz, C10/13), 74.4 (d, $^3J_{CP}$ = 6.1 Hz, C11/12), 74.9 (d, $^2J_{CP}$ = 14.0 Hz, C10/13), 78.8 (d, $^1J_{CP}$ = 44.0 Hz, C14), 84.6 (d, $^2J_{CP}$ = 3.6 Hz, C45/C46), 86.2 (d, $^2J_{CP}$ = 7.0 Hz, C45/C46), 86.6 (s, C5), 89.1 (d, $^2J_{CP}$ = 2.7 Hz, C43/C44), 90.8 (d, $^2J_{CP}$ = 2.2 Hz, C43/C44), 95.0 (d, $^2J_{CP}$ = 4.4 Hz, C42), 108.2 (s, C47), 121.8 (s, C30), 122.1 (d, $^3J_{CP}$ = 4.1 Hz, C2), 122.4 (d, $^3J_{CP}$ = 3.8 Hz, C36), 128.1 (s, C3), 128.6 (d, $^3J_{CP}$ = 9.3 Hz, C17), 129.0 (s, C31), 129.1 (s, C37), 130.7 (s, C18), 132.9 (d, $^2J_{CP}$ = 8.3 Hz, C16), 133.2 (s, C32, C38), 134.9 (d, $^1J_{CP}$ = 40.1 Hz, C15), 135.9 (s, C4), 139.8 (d, $^3J_{CP}$ = 13.9 Hz, C39), 140.2 (d, $^3J_{CP}$ = 11.3 Hz, C33), 149.9 (d, $^2J_{CP}$ = 6.9 Hz, C1), 151.8 (s, C35), 151.9 (s, C29). $^{31}P\{^1H\}$-NMR (162.0 MHz, CD_2Cl_2): δ (ppm) = 8.2 (s, N_3P_3), 15.0 (br s, (*R*)-P-Ru), 62.6 (s, P=S).

Electrochemistry

All electrochemical measurements were conducted at room temperature with a Biologic Science Instruments SP-50 potentiostat using a three-electrode cell setup from Gamry Instruments equipped with a glassy carbon working electrode, a platinum counter electrode and a non-aqueous Ag/Ag^+ reference electrode (0.01 mol L^{-1} $AgNO_3$, 0.1 mol L^{-1} [*n*Bu_4N][PF_6] in acetonitrile). Decamethylferrocene ($E_{1/2}$ = –0.55 V vs. FcH/FcH^+) was used as internal standard and all half-wave potentials were referenced vs. ferrocene. The compounds were dissolved in DCM under nitrogen atmosphere with 0.1 mol L^{-1} [*n*Bu_4N][PF_6] electrolyte prior to each measurement.

Catalytic Transformation

General Procedure for Transfer Hydrogenation of Acetophenone. A Schlenk flask containing the ruthenium precursor (1.0 mol-% Ru) was evacuated and filled with nitrogen three times. A stock solution (6.5 mL) of potassium *tert*-butoxide (7.7 mmol L^{-1}) in THF was added and the solution was preheated at 85 °C for 10 minutes. To start the catalytic run, a stock solution (6.5 mL) of acetophenone (77.0 mmol L^{-1}) and anisole (77.0 mmol L^{-1}) in 2-propanol was quickly added. The yield of (*R*)/(*S*)-1-phenylethanol was monitored by GC-MS analysis taking samples at the allotted times (30 μL diluted with 1.5 mL of acetone).

Redox-Switchable Transfer Hydrogenation. A Schlenk flask containing the ruthenium precursor (1.0 mol-% Ru) was evacuated and filled with nitrogen three times. A stock solution (6.5 mL) of potassium *tert*-butoxide (7.7 mmol L^{-1}) in THF was added and the solution was preheated at 85 °C for 10 minutes. To start the catalytic run, a stock solution (6.5 mL) of acetophenone (77.0 mmol L^{-1}) and anisole (77.0 mmol L^{-1}) in 2-propanol was quickly added. At a certain point, the oxidant acetylferrocenium tetrafluoroborate (1.0 mol-%), dissolved in THF (0.005 mol L^{-1}), was added to the reaction. For the reduction, a solution of decamethylferrocene (1.1 mol-%) in THF (0.005 mol L^{-1}) was added. The yield of (*R*)/(*S*)-1-phenylethanol was monitored by GC-MS analysis taking samples at the allotted times (30 μL diluted with 1.5 mL of acetone).

X-ray Crystallography

Data reduction was performed with CrysAlis Pro[76] including the program SCALE3 ABSPACK[77] for empirical absorption correction. Structures were solved by direct methods and refined by full-matrix least-squares techniques against F^2 with the SHELX program package.[78] All non-hydrogen atoms were refined with anisotropic thermal parameters and all non-boron-bonded hydrogen atoms were assigned riding isotropic displacement parameters and constrained to idealized geometries. Structure figures were generated with Mercury 4.0.0.[79,80]

CCDC 1960781 (for **1a**), 1960783 (for **2a**), and 1960782 (for **3b**) contain the supplementary crystallographic data for this paper. These data can be obtained free of charge from The Cambridge Crystallographic Data Centre.

Acknowledgments

Financial support of the EU COST Action CM1302 Smart Inorganic Polymers (SIPs) and the Graduate School BuildMoNa is gratefully acknowledged. Furthermore, we thank Dr. P. Lönnecke for X-ray data collection on single crystals.

Keywords: Asymmetric catalysis · Dendrimers · Homogeneous catalysis · Phosphines · Redox-switchable catalysis

[1] A. M. Allgeier, C. A. Mirkin, *Angew. Chem. Int. Ed.* **1998**, *37*, 894–908; *Angew. Chem.* **1998**, *110*, 936–952.
[2] V. Lyaskovskyy, B. De Bruin, *ACS Catal.* **2012**, *2*, 270–279.
[3] I. M. Lorkovic, R. R. Duff, M. S. Wrighton, *J. Am. Chem. Soc.* **1995**, *117*, 3617–3618.
[4] O. R. Luca, R. H. Crabtree, *Chem. Soc. Rev.* **2013**, *42*, 1440–1459.
[5] V. Blanco, D. A. Leigh, V. Marcos, *Chem. Soc. Rev.* **2015**, *44*, 5341–5370.
[6] A. J. Teator, D. N. Lastovickova, C. W. Bielawski, *Chem. Rev.* **2016**, *116*, 1969–1992.
[7] C. Chen, *ACS Catal.* **2018**, *8*, 5506–5514.
[8] E. Peris, *Chem. Rev.* **2018**, *118*, 9988–10031.
[9] J. Choudhury, *Tetrahedron Lett.* **2018**, *59*, 487–495.
[10] Y. Ryu, G. Ahumada, C. W. Bielawski, *Chem. Commun.* **2019**, *55*, 4451–4466.
[11] C. K. A. Gregson, V. C. Gibson, N. J. Long, E. L. Marshall, P. J. Oxford, A. J. P. White, *J. Am. Chem. Soc.* **2006**, *128*, 7410–7411.
[12] E. M. Broderick, P. S. Thuy-Boun, N. Guo, C. S. Vogel, J. Sutter, J. T. Miller, K. Meyer, P. L. Diaconescu, *Inorg. Chem.* **2011**, *50*, 2870–2877.
[13] E. M. Broderick, N. Guo, C. S. Vogel, C. Xu, J. Sutter, J. T. Miller, K. Meyer, P. Mehrkhodavandi, P. L. Diaconescu, *J. Am. Chem. Soc.* **2011**, *133*, 9278–9281.

[14] C. D. Varnado, E. L. Rosen, M. S. Collins, V. M. Lynch, C. W. Bielawski, *Dalton Trans.* **2013**, *42*, 13251–13264.
[15] R. Savka, S. Foro, M. Gallei, M. Rehahn, H. Plenio, *Chem. Eur. J.* **2013**, *19*, 10655–10662.
[16] S. M. Guillaume, E. Kirillov, Y. Sarazin, J. F. Carpentier, *Chem. Eur. J.* **2015**, *21*, 7988–8003.
[17] J. Wei, P. L. Diaconescu, *Acc. Chem. Res.* **2019**, *52*, 415–424.
[18] G. Liu, H. He, J. Wang, *Adv. Synth. Catal.* **2009**, *351*, 1610–1620.
[19] K. Arumugam, C. D. Varnado, S. Sproules, V. M. Lynch, C. W. Bielawski, *Chem. Eur. J.* **2013**, *19*, 10866–10875.
[20] L. Hettmanczyk, S. Manck, C. Hoyer, S. Hohloch, B. Sarkar, *Chem. Commun.* **2015**, *51*, 10949–10952.
[21] S. Ibáñez, M. Poyatos, L. N. Dawe, D. Gusev, E. Peris, *Organometallics* **2016**, *35*, 2747–2758.
[22] L. Hettmanczyk, L. Suntrup, S. Klenk, C. Hoyer, B. Sarkar, *Chem. Eur. J.* **2017**, *23*, 576–585.
[23] A. Feyrer, M. K. Armbruster, K. Fink, F. Breher, *Chem. Eur. J.* **2017**, *23*, 7402–7408.
[24] A. Feyrer, F. Breher, *Inorg. Chem. Front.* **2017**, *4*, 1125–1134.
[25] S. Klenk, S. Rupf, L. Suntrup, M. Van Der Meer, B. Sarkar, *Organometallics* **2017**, *36*, 2026–2035.
[26] B. L. Thompson, C. R. Simons, Z. M. Heiden, *Chem. Commun.* **2019**, *55*, 11430–11433.
[27] P. Veit, C. Volkert, C. Förster, V. Ksenofontov, S. Schlicher, M. Bauer, K. Heinze, *Chem. Commun.* **2019**, *55*, 4615–4618.
[28] S. Ibáñez, M. Poyatos, E. Peris, *ChemCatChem* **2016**, *8*, 3790–3795.
[29] D. Wang, D. Astruc, *Chem. Rev.* **2015**, *115*, 6621–6686.
[30] G. Brieger, T. J. Nestrick, *Chem. Rev.* **1974**, *74*, 567–580.
[31] G. Zassinovich, G. Mestroni, S. Giadiali, *Chem. Rev.* **1992**, *92*, 1051–1069.
[32] R. Noyori, S. Hashiguchi, *Acc. Chem. Res.* **1997**, *30*, 97–102.
[33] M. J. Palmer, M. Wills, *Tetrahedron: Asymmetry* **1999**, *10*, 2045–2061.
[34] K. Everaere, A. Mortreux, J.-F. Carpentier, *Adv. Synth. Catal.* **2003**, *345*, 67–77.
[35] S. Gladiali, E. Alberico, *Chem. Soc. Rev.* **2006**, *35*, 226–236.
[36] T. Ikariya, A. J. Blacker, *Acc. Chem. Res.* **2007**, *40*, 1300–1308.
[37] C. Wang, X. Wu, J. Xiao, *Chem. Asian J.* **2008**, *3*, 1750–1770.
[38] F. Foubelo, C. Nájera, M. Yus, *Tetrahedron: Asymmetry* **2015**, *26*, 769–790.
[39] C. Diez, U. Nagel, *Appl. Organomet. Chem.* **2010**, *24*, 509–516.
[40] K. Yoshida, T. Kamimura, H. Kuwabara, A. Yanagisawa, *Chem. Commun.* **2015**, *51*, 15442–15445.
[41] B. Ramasamy, M. Kumar Gangwar, P. Ghosh, *Eur. J. Inorg. Chem.* **2017**, *2017*, 3253–3268.
[42] Y. Li, M. Lei, W. Yuan, E. Meggers, L. Gong, *Chem. Commun.* **2017**, *53*, 8089–8092.
[43] S. Hashiguchi, A. Fujii, J. Takehara, T. Ikariya, R. Noyori, *J. Am. Chem. Soc.* **1995**, *117*, 7562–7563.
[44] T. Ohkuma, H. Ooka, S. Hashiguchi, T. Ikariya, R. Noyori, *J. Am. Chem. Soc.* **1995**, *117*, 2675–2676.
[45] A. Fujii, S. Hashiguchi, N. Uematsu, T. Ikariya, R. Noyori, *J. Am. Chem. Soc.* **1996**, *118*, 2521–2522.
[46] K. J. Haack, S. Hashiguchi, A. Fujii, T. Ikariya, R. Noyori, *Angew. Chem. Int. Ed. Engl.* **1997**, *36*, 285–288; *Angew. Chem.* **1997**, *109*, 297–300.
[47] K. Matsumura, S. Hashiguchi, T. Ikariya, R. Noyori, *J. Am. Chem. Soc.* **1997**, *119*, 8738–8739.
[48] J. Takehara, S. Hashiguchi, A. Fujii, S. I. Inoue, T. Ikariya, R. Noyori, *Chem. Commun.* **1996**, 233–234.
[49] D. A. Alonso, P. Brandt, S. J. M. Nordin, P. G. Andersson, *J. Am. Chem. Soc.* **1999**, *121*, 9580–9588.
[50] J. P. Genêt, V. Ratovelomanana-Vidal, C. Pinel, *Synlett* **1993**, 478–480.
[51] P. Barbaro, C. Bianchini, A. Togni, *Organometallics* **1997**, *16*, 3004–3014.
[52] G. A. Carriedo, P. Crochet, F. J. G. Alonso, J. Gimeno, A. Presa-Soto, *Eur. J. Inorg. Chem.* **2004**, 3668–3674.
[53] A. Grabulosa, J. Granell, G. Muller, *Coord. Chem. Rev.* **2007**, *251*, 25–90.
[54] A. Grabulosa, J. J. Spivey, *P-Stereogenic Ligands in Enantioselective Catalysis*, The Royal Society of Chemistry, **2011**.
[55] O. I. Kolodiazhnyi, *Tetrahedron: Asymmetry* **2012**, *23*, 1–46.
[56] A. Grabulosa, A. Mannu, A. Mezzetti, G. Muller, *J. Organomet. Chem.* **2012**, *696*, 4221–4228.
[57] A. Grabulosa, A. Mannu, E. Alberico, S. Denurra, S. Gladiali, G. Muller, *J. Mol. Catal. A* **2012**, *363–364*, 49–57.
[58] R. Aznar, A. Grabulosa, A. Mannu, G. Muller, D. Sainz, V. Moreno, M. Font-Bardia, T. Calvet, J. Lorenzo, *Organometallics* **2013**, *32*, 2344–2362.
[59] P. Clavero, A. Grabulosa, M. Font-Bardia, G. Muller, *J. Mol. Catal. A* **2014**, *391*, 183–190.
[60] L.-I. Rodriguez, O. Rossell, M. Seco, G. Muller, *J. Organomet. Chem.* **2007**, *692*, 851–858.
[61] R. Van Heerbeek, P. C. J. Kamer, P. W. N. M. Van Leeuwen, J. N. H. Reek, *Chem. Rev.* **2002**, *102*, 3717–3756.
[62] A. Ouali, A.-M. Caminade, R. Laurent, in *Dendrimers Towards Catalytic, Material and Biomedical Uses*, John Wiley & Sons Ltd. **2011**, pp. 163–265.
[63] R. Laurent, A.-M. Caminade, J.-P. Majoral, *Tetrahedron Lett.* **2005**, *46*, 6503–6506.
[64] A.-M. Caminade, A. Ouali, R. Laurent, C.-O. Turrin, J.-P. Majoral, *Chem. Soc. Rev.* **2015**, *44*, 3890–3899.
[65] P. Neumann, H. Dib, A.-M. Caminade, E. Hey-Hawkins, *Angew. Chem. Int. Ed.* **2015**, *54*, 311–314; *Angew. Chem.* **2015**, *127*, 316-319.
[66] J.-P. Majoral, A.-M. Caminade, *Chem. Rev.* **1999**, *99*, 845–880.
[67] J. Popp, S. Hanf, E. Hey-Hawkins, *ACS Omega* **2019**, *4*, 22540–22548.
[68] J. Popp, S. Hanf, E. Hey-Hawkins, *Chem Eur. J.* **2020**, accepted, DOI: 10.1002/chem.202000218
[69] P. Neumann, H. Dib, A. Sournia-Saquet, T. Grell, M. Handke, A.-M. Caminade, E. Hey-Hawkins, *Chem. Eur. J.* **2015**, *21*, 6590–6604.
[70] S. Jugé, M. Stephan, J. A. Laffitte, J. P. Genet, *Tetrahedron Lett.* **1990**, *31*, 6357–6360.
[71] N. Launay, A.-M. Caminade, J.-P. Majoral, *J. Organomet. Chem.* **1997**, *529*, 51–58.
[72] N. G. Connelly, W. E. Geiger, *Chem. Rev.* **1996**, *96*, 877–910.
[73] M. Navarro, D. Vidal, P. Clavero, A. Grabulosa, G. Muller, *Organometallics* **2015**, *34*, 973–994.
[74] L. Wang, Q. Yang, H.-Y. Fu, H. Chen, M.-L. Yuan, R.-X. Li, *Appl. Organomet. Chem.* **2011**, *25*, 626–631.
[75] M. S. Inkpen, S. Du, M. Driver, T. Albrecht, N. J. Long, *Dalton Trans.* **2013**, *42*, 2813–2816.
[76] *CrysAlis Pro*: Data Collection and Data Reduction Software Package, Agilent Technologies.
[77] *SCALE3 ABSPACK*: Empirical Absorption Correction Using Spherical Harmonics.
[78] G. M. Sheldrick, *Acta Crystallogr., Sect. A Found. Crystallogr.* **2008**, *64*, 112–122.
[79] C. F. Macrae, P. R. Edgington, P. McCabe, E. Pidcock, G. P. Shields, R. Taylor, M. Towler, J. van de Streek, *J. Appl. Crystallogr.* **2006**, *39*, 453–457.
[80] C. F. Macrae, I. J. Bruno, J. A. Chisholm, P. R. Edgington, P. McCabe, E. Pidcock, L. Rodriguez-Monge, R. Taylor, J. van de Streek, P. A. Wood, *J. Appl. Crystallogr.* **2008**, *41*, 466–470.

Received: February 11, 2020